



UNIVERSIDADE FEDERAL DO RIO DE JANEIRO
INSTITUTO DE FÍSICA

Experimental Distillation of Quantum Steering

Paulo Eduardo de Almeida Vale Silva Sahium

Dissertação de Mestrado apresentada ao Programa de Pós-Graduação em Física do Instituto de Física da Universidade Federal do Rio de Janeiro - UFRJ, como parte dos requisitos necessários à obtenção do título de Mestre em Ciências (Física).

Orientador: Stephen Patrick Walborn

Co-orientadora: Malena Osorio Hor-Meyll

Rio de Janeiro
Setembro de 2017

d96e de Almeida Vale Silva Sahium, Paulo Eduardo
Experimental Distillation of Quantum Steering /
Paulo Eduardo de Almeida Vale Silva Sahium. -- Rio
de Janeiro, 2017.
64 f.

Orientador: Stephen Patrick Walborn.
Coorientadora: Malena Osorio Hor-Meyll.
Dissertação (mestrado) - Universidade Federal do
Rio de Janeiro, Instituto de Física, Programa de Pós
Graduação em Física, 2017.

1. Correlações quânticas. 2. Steering. 3.
Destilação. 4. Distribuição de chaves. I. Patrick
Walborn, Stephen, orient. II. Osorio Hor-Meyll,
Malena, coorient. III. Título.

Experimental Distillation of Quantum Steering

Paulo Eduardo de Almeida Vale Silva Sahium

Stephen Patrick Walborn
Malena Osório Hor-Meyll

Dissertação de Mestrado submetida ao Programa de Pós-Graduação em Física, Instituto de Física, da Universidade Federal do Rio de Janeiro – UFRJ, como parte dos requisitos necessários à obtenção do título de Mestre em Ciências (Física).

Aprovada por:



Stephen Patrick Walborn
(Presidente e Orientador)



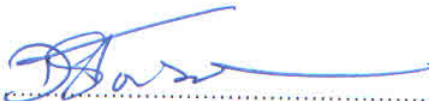
Malena Osório Hor-Meyll
(Co-Orientador)



Marcelo Paleólogo Elefteriadis de França Santos



François Impens



Daniel Schneider Tasca

Resumo

Destilação Experimental de Steering Quântico

Paulo Eduardo de Almeida Vale Silva Sahium

Orientador: Stephen Patrick Walborn

Co-orientadora: Malena Osorio Hor-Meyll

Resumo da Dissertação de Mestrado submetida ao Programa de Pós-graduação em Física, Instituto de Física, da Universidade Federal do Rio de Janeiro - UFRJ, como parte dos requisitos necessários à obtenção do título de Mestre em Ciências (Física)

Destilação é um processo em que ocorre um incremento na quantidade de uma propriedade em questão. Especificamente, fazemos o uso de uma teoria de recursos para steering para executar a destilação. Uma teoria de recursos define transformações permitidas em um sistema com a finalidade de obter vantagens para alguma aplicação. A teoria de recursos para o emaranhamento foi desenvolvida desde 1998, assim como quantificadores de emaranhamento, fornecendo os requisitos necessários para a destilação. Em 2001, Kwiat *et al.* [Nature 409 (2001)] realizou o primeiro experimento demonstrando a destilação do emaranhamento.

Por outro lado, “steering”, uma propriedade introduzida em 1935, foi apenas recentemente desenvolvida com maiores detalhes. Ela se caracteriza pela capacidade aparente de um sistema quântico de “conduzir” o sistema do outro em um ensemble distinto de estados, e foi classificada como sendo intermediária ao emaranhamento e não-localidade de Bell. Uma teoria de recursos para o steering e seus quantificadores já foram introduzidos. Porém, um protocolo para a destilação e a realização experimental ainda não foram feitos. Nesta dissertação, descrevemos um protocolo com o objetivo de destilar steering e também o realizamos experimentalmente utilizando fótons com informação codificada em dois graus de liberdade: momento e polarização. A operação utilizada no protocolo foi a “One Sided Local Operations with Classical Communication”, descrita pela teoria de recursos como uma das operações permitidos para o steering.

Nosso resultado demonstra a destilação do steering para um estado e, ao final, discutimos a importância deste resultado frente a aplicações em informação quântica. Além disto, comentamos sobre trabalhos futuros que podem ser realizados a partir deste.

Palavras-chave: 1. Correlações quânticas 2. Steering 3. Destilação 4. Distribuição de chaves quânticas

Rio de Janeiro
Setembro de 2017

Abstract

Experimental Distillation of Quantum Steering

Paulo Eduardo de Almeida Vale Silva Sahium

Orientador: Stephen Patrick Walborn

Co-orientadora: Malena Osorio Hor-Meyll

Abstract da Dissertação de Mestrado submetida ao Programa de Pós-graduação em Física, Instituto de Física, da Universidade Federal do Rio de Janeiro - UFRJ, como parte dos requisitos necessários à obtenção do título de Mestre em Ciências (Física)

Distillation is a process in which there is an increase in the amount of a property in question. Specifically, we make use of a resource theory description for steering to achieve distillation. A resource theory defines the allowable transformations that can be applied on a system in order to take advantage of it for applications.

Entanglement resource theory has been developed since 1998 as well as entanglement quantifiers, providing the necessary requirements for distillation to be introduced. In 2001, a first experiment was performed by Kwiat *et al.* [Nature 409 (2001)] showing experimental entanglement distillation.

On the other hand, steering, which was first suggested in 1935, was only recently defined more rigorously as a distinct quantum correlation. It is the apparent ability of one quantum system to “steer” the quantum state of another system into distinct ensembles of states, and is placed as an intermediate correlation between entanglement and Bell-nonlocality. A steering resource theory, as well as steering quantifiers, were already introduced but a distillation procedure and experiment has not yet been performed. In this dissertation, we describe a protocol to achieve steering distillation and perform the experiment using photon-encoded information in two different degrees of freedom, momentum and polarization. The general operation used to perform the distillation is “One Sided Local Operations with Classical Communications”, described by resource theory as the allowed operations for steering.

Our result show steering distillation for some states and, at the end, we discuss the importance of such result regarding applications in quantum information. Also, we comment about an extension of this work for a future research.

Key-words: 1. Quantum correlation 2. Steering 3. Distillation 4. One Sided Device Independent Quantum Key Distribution

Rio de Janeiro
Setembro de 2017

Acknowledgement

Primarily I am thankful to God for all his support and provision throughout all of my studies. His guidance along this way was of essential importance, as well as the strength to overcome every difficulty presented to me. I thank my parents, Mirian and Paulo Henrique, for always encouraging me to do what I like and for backing me on my decision to do a masters in physics. Also, I am truly grateful to Louise Marie, my fiancé, whom have stood before me all this time, being supportive and comprehensive at all times.

I thank both my supervisors, Stephen Patrick Walborn and Malena Osorio Hor-Meyll, for accepting me as their student and for believing I could develop this research, despite my background not being in physics, but in biology. The majority of knowledge I have in physics today is due to their contribution, where both have always been attentive and patient while listening my questions, as well as while answering them.

I cannot forget to thank my group colleagues Álvaro Pimentel, Carolina Gigliotti, Eduardo Paul, Gabo, Kei Sawada, Matheus Esteves, Otávio Cals, Ranieri Neri, Renato Mello and Thais Silva whom shared this journey with me and were always there when I had difficulties on any discipline. I thank them sharing their lunch time at the laboratory with me, where we regularly had a great time together. I am really grateful for being part of such an integrated group, where there is always a good atmosphere and no dispute among the members, except when there is chocolate.

I specifically thank Gabo for his contributions towards overcoming complications we had while building the experiment, without his ideas and expertise we would not have concluded the experiment in the time we did. I thank him for his encouragement to not be afraid of rebuilding parts of the experiment and for providing motivation to finish it. Not only that, his advices regarding my studies were very welcome and beneficial.

Specially, I am grateful for Ranieri Vieira Neri help in developing the entire project. Our alternating schedule of who was working at the experiment certainly reduced our completion time. His knowledge about the used experimental techniques and MatLAB programming language were

crucial to integrate the measurements performed with the data analysis. Besides that, his awareness of steering theory was of immense help and certainly made the difference in my development, as he was always kind to answer any question I presented him.

Finally, but not less important, I acknowledge the Physics Institute for their efficient work and communication with the students, and I am thankful for the learning I had as a member of the Post-Graduate Committee. Also, I acknowledge and thank the funding support received by the Brazilian National Council for Scientific and Technological Development (CNPq), the Foundation for Research Support of the State of Rio de Janeiro (FAPERJ), the Coordination for the Improvement of Higher Education Personnel (CAPES) and the Brazilian National Institute for Science and Technology of Quantum Information (INCT-IQ), which may not have directly supported me, but did it indirectly, by supporting the projects I took part in.

Summary

1	Introduction	1
2	Fundamental Concepts	5
2.1	Qubits	5
2.2	Density matrix	7
2.3	Generation of entangled states	9
2.4	State operations	13
2.4.1	Waveplates	13
2.4.2	Beam displacer	14
2.4.3	Beam splitter	16
2.5	State measurement	17
2.6	State reconstruction	20
3	Steering	22
3.1	Theory	22
3.2	Steering operations	26
3.3	Steering quantifier	28
3.4	Steering distillation	30
4	The experiment	32
4.1	Experimental implementation	32
4.2	Data processing and analysis	39
5	Conclusion and remarks on future work	47
	References	48
A	Measurement outcome	53

B Equipment

Chapter 1

Introduction

Can a quantum state, which exhibits a quantum correlation, have this correlation increased by a classical user? This is the question that guides the present work and we give an answer to it considering one specific type of correlation.

One of the most known and studied quantum correlations to date is entanglement, which occurs when a certain group of quantum particles that interacted or were created together share a deeply connection, no matter the distance these particles are from one another. This strange phenomenon intrigued physicists at the beginning of the twentieth century (and still intrigues) and made them question if the quantum mechanical description of nature was correct [1].

In 1964 J. S. Bell [2] shed light on this problem by defining mathematically an inequality that, if violated, would confirm that nature indeed exhibits this correlation known as quantum entanglement, as predicted by quantum theory. This allowed not only for a confirmation of the theory, but also a way to test for entanglement in quantum states. It turned out that only some entangled quantum states violated this inequality. It was in 1989, in an article by R. Werner [3], that this difference became more clear. He defined more precisely the concept of entanglement, or non-separability, which, for a bipartite system, is a state that cannot be written as

$$W = \sum_i p_i \sigma^A \otimes \rho^B \tag{1.1}$$

where p_i are the elements of a positive probability distribution, σ^A is the state of one of the parties and ρ^B is the state of the other party. A state that can be written in this form is said to be separable, or not entangled. This is a description that covered all entangled states, therefore, it

became a criteria used to identify entanglement, while the inequality derived by Bell serves to characterize a strict set of entangled states, which became known as Bell non-local states. Since then, a resource theory [4] and quantifiers [5,6] were introduced for entanglement.

Another known correlation that is similar to entanglement and Bell non-locality is steering. It was first suggested in 1935 [7], but was also misunderstood as entanglement. The distinction was made by H. M. Wiseman *et al* [8], as we shall see in more detail in the course of this dissertation, but mainly it can be understood as an intermediate correlation between entanglement and Bell non-locality. For instance, entanglement is treated as a property between two parties where knowledge is required about both systems measurement devices (white boxes in Figure 1.1a). In Bell non-locality, on the other hand, the measurement devices are not trustworthy and no assumptions can be made about them or the physical systems they act upon, configuring a scheme of black-boxes (see Figure 1.1c). Indeed, no knowledge about quantum physics is required to derive Bell non-locality. Steering is a type of hybrid correlation, requiring knowledge about one of the systems devices, but no knowledge about the other.

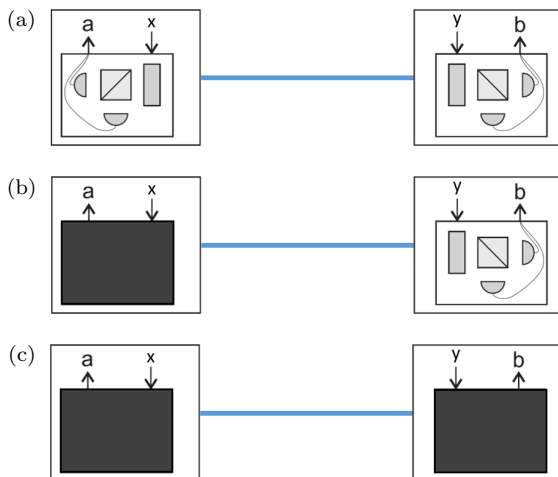


Figure 1.1: **Black boxes representation for entanglement, steering and Bell non-locality.** (a) entanglement, (b) steering and (c) Bell non-locality. Image adapted from [9].

Like entanglement, a resource theory [10] and quantifiers [11,12] were developed for steering after it was characterised.

All of these properties have important applications. As an example, entanglement can be used for superdense coding [13], quantum teleportation [14], quantum cryptography [15–17], and Standard Quantum Key Distribution (S-QKD) [15]. Bell non-locality is useful for reducing communication complexity in some classical communication tasks [18] as well as Device Independent Quantum Key Distribution (DI-QKD) [19]. Steering, as an intermediate type of correlation, has

been proposed as a resource for One Side Device Independent Quantum Key Distribution (1s DI-QKD) [9]. The identification of quantum information tasks that require each of these respective resources for successful operation is an exciting ongoing line of research.

A common application for all of the above correlations is QKD. QKD is a process that allows two parties, Alice and Bob, to establish a shared secret key which can be used to encrypt and decrypt messages. Each correlation places a different security requirement to establish this key. S-QKD security is guaranteed under the assumption that Alice and Bob trust their preparation and measurement devices. In a different way, in DI-QKD both measurement apparatuses are treated as untrusted black-boxes. The intermediate case, 1s DI-QKD, requires that only Bob's measurements be trustworthy, while Alice's is not. S-QKD does not reflect reality, since there can always be a malefactor trying to eavesdrop on the communication. DI-QKD and 1s DI-QKD looks like realistic scenarios, with the former being the ideal one. However, the real world implementation is easier for 1s DI-QKD [20, 21].

The above applications rely on the capacity of sharing pairs of correlated systems between two distant parties. This is not an easy task, since the quality of such states tend to decrease as they travel through a quantum channel. A way to surpass this problem is known as distillation and has been shown for entangled states [22]. Entanglement distillation consists of the transformation of N copies of non-maximally entangled states into a smaller number ($< N$) of near maximally entangled states, using Local Operations and Classical Communication (LOCC). Distillation thus plays an important role towards the feasibility of QKD and other processes, but had not been demonstrated for steering until now.

In this work we experimentally investigate a distillation protocol for steering, using a similar approach to that for entanglement. The difference lies on the allowed operations described by their respective resource theory. For entanglement there is LOCC, while for steering we have the One Way Local Operations with Classical Communications (1W-LOCC's). As the name suggests, one of the parties is allowed to perform local operations and communicate with the other party, while the inverse is not permitted. This reinforces the view of steering as a composition of one white box, the one that is allowed to perform local operations, and one black box.

In order to perform the experiment we use two copies of entangled qubits with a certain amount of steering at the beginning. The two pairs of entangled qubits are encoded into different degrees of freedom of a single pair of photons. This type of dual entanglement is called hyper-entanglement [23, 24]. Then, with the action of a local filtering, we increase the steerability of the states. In contrast to single-copy local filtering, our protocol is deterministic, in the sense that Alice and Bob always have an entangled pair of qubits for each run of the protocol. At the end, our results show

that it is possible to distill steering.

The structure of this dissertation is as follows: In the second chapter the general concepts needed to understand this work are presented. First we will see a description of a qubit, how to mathematically represent a quantum state, and how entangled states can be generated. Then, follows a review on the types of experimental devices used to manipulate a state that are relevant to this experiment. These are waveplates, beam displacers and beam splitters. In the last part of this chapter is a description of how a measurement is performed and how these measurements can be combined to recover information about a state.

The third chapter contains a detailed explanation on how to characterise three quantum properties - entanglement, steering and Bell non-locality - using probability theory, with a specific focus on steering. A description of steering as a resource theory is provided and the type of operations we are allowed to perform, as well as how to quantify it. At last follows a process on how to increase the amount of resource present on an ensemble of states (distillation).

The first part of the fourth chapter describes the experimental setup used to perform steering distillation, giving detailed information on each experimental device. The second part presents our results and data analysis. Finally, in the last chapter we present the conclusion of this work and remarks on future prospects.

Chapter 2

Fundamental Concepts

Photons, the elementary particles of light, are being used for several applications, like quantum communications, quantum computing, quantum teleportation and quantum metrology. These applications take advantage of particles that in the quantum regime present very interesting and useful characteristics and properties. Despite the fact that quantum theory has been around for more than a hundred years, some aspects are still being discovered and characterized. Steering is one of them, and the present work makes use of photons to demonstrate the distillation of Steering.

Understanding how to describe, generate and manipulate photon states is therefore essential for exploring light applications in the quantum domain. What follows in this chapter is a review on photonic qubits, how to generate entangled pairs of photons and how to manipulate, measure and analyse these states.

2.1 Qubits

The quantum bit (qubit) is the fundamental element of quantum information and quantum computation, like the bit is for classical computation. A qubit is a two-level quantum system with states 0 or 1, like its classical counterpart, but it also has the possibility to exist as a linear combination of these states, called a superposition state:

$$|\psi\rangle = \alpha |0\rangle + \beta |1\rangle, \quad (2.1)$$

where α and β are complex numbers. Many systems can be described using this notation, such as the spin of a particle or the energy levels of an atom, but in this work I will focus mostly on the qubit as the polarization degree of freedom. Polarization is the direction that the electromagnetic field oscillates and in this case the states of the computational basis, $|0\rangle$ and $|1\rangle$, can be represented by $|H\rangle$ and $|V\rangle$, respectively, with H meaning horizontal polarization and V vertical polarization. Their matrix form is

$$|0\rangle = |H\rangle = \begin{pmatrix} 1 \\ 0 \end{pmatrix} ; |1\rangle = |V\rangle = \begin{pmatrix} 0 \\ 1 \end{pmatrix}. \quad (2.2)$$

The state vector representation [Equation (2.1)] may look simple at first sight, but when measurement is taken into account an intriguing phenomena arises. The result of a measurement in the $\{0/1\}$ basis will not be a superposition state, instead it will be either $|0\rangle$, with probability $|\alpha|^2$, or $|1\rangle$, with probability $|\beta|^2$. These probabilities must sum to one, therefore $|\alpha|^2 + |\beta|^2 = 1$. Under this normalization condition one interpretation for the state is that of a unit vector spanned over a two-dimensional Hilbert space, where the Hilbert space \mathcal{H} is a vector space containing the structure of an inner product, allowing the measurement of lengths and angles. One useful picture of the vector arises by rewriting Equation (2.1) as:

$$|\psi\rangle = \cos \theta/2 |0\rangle + e^{i\varphi} \sin \theta/2 |1\rangle, \quad (2.3)$$

where θ and φ are angles in a three-dimensional sphere (see Figure 2.1), with $0 \leq \theta \leq \pi$ and $0 \leq \varphi \leq 2\pi$. The sphere is called *Bloch Sphere*, or *Poincaré Sphere* for light polarization, and is a powerful tool to visualize operations applied on a single qubit. Some points of the sphere surface with unitary radius represent important states, the z-axis represents the computational base states $|0\rangle$ and $|1\rangle$, while the equator represents maximal superposition states in the same basis. The positive and negative extremes of the x-axis represent $(|0\rangle + |1\rangle)/\sqrt{2}$ and $(|0\rangle - |1\rangle)/\sqrt{2}$ states, respectively, and the positive and negative extremes of the y-axis represent $(|0\rangle + i |1\rangle)/\sqrt{2}$ and $(|0\rangle - i |1\rangle)/\sqrt{2}$, respectively. These superposition states can be written in terms of linear polarizations, where the positive and negative part of the x-axis becomes diagonal ($|D\rangle$) and anti-diagonal ($|A\rangle$) polarizations, respectively, and the positive and negative part of the y-axis becomes right circular ($|R\rangle$) and left circular ($|L\rangle$) polarizations, with

$$\begin{aligned}
|D\rangle &= \frac{|H\rangle + |V\rangle}{\sqrt{2}} \quad , \quad |A\rangle = \frac{|H\rangle - |V\rangle}{\sqrt{2}}, \\
|R\rangle &= \frac{|H\rangle + i|V\rangle}{\sqrt{2}} \quad , \quad |L\rangle = \frac{|H\rangle - i|V\rangle}{\sqrt{2}}.
\end{aligned}
\tag{2.4}$$

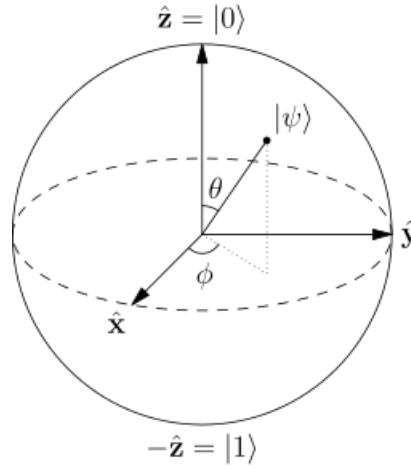


Figure 2.1: **Bloch Sphere with a unitary vector representing a state.** The positive and negative part of x -axis can be identified with the diagonal ($|D\rangle$) and anti-diagonal ($|A\rangle$) states, respectively. Also, the positive and negative part of y -axis can be identified with the right ($|R\rangle$) and left ($|L\rangle$) circularly polarized states. Image taken from www.wikipedia.com

2.2 Density matrix

The formulation of quantum mechanics via the state vector is useful, however, it is not always possible to describe a two-level system using (2.1). There exists an extension that makes characterization and description of all systems possible, that is the *density matrix* formulation. While the state vector formulation is adequate for describing pure states, the density operator is useful for describing an ensemble of pure states, namely mixed states, and is defined as

$$\rho \equiv \sum_i p_i |\psi_i\rangle \langle \psi_i|,
\tag{2.5}$$

where i is an index and p_i are probabilities. Each term inside the sum is an outer product, or a *projector* that can be written as $\mu_i = |\psi_i\rangle \langle \psi_i|$.

In general, the density matrix of any two-level system will be a 2x2 matrix that can be decom-

posed in a combination of four matrices that form a basis:

$$\rho = \frac{1}{2}(\mathbb{1} + \vec{r} \cdot \vec{\sigma}) \quad (2.6)$$

with $\mathbb{1}$ being the identity matrix, $\vec{r} = (r_1, r_2, r_3)$ a unit vector on the Bloch sphere and $\vec{\sigma} = (\sigma_x, \sigma_y, \sigma_z)$ are the Pauli matrices¹, defined as

$$\mathbb{1} = \begin{pmatrix} 1 & 0 \\ 0 & 1 \end{pmatrix} \quad ; \quad \sigma_x = \begin{pmatrix} 0 & 1 \\ 1 & 0 \end{pmatrix} \quad ; \quad \sigma_y = \begin{pmatrix} 0 & -i \\ i & 0 \end{pmatrix} \quad ; \quad \sigma_z = \begin{pmatrix} 1 & 0 \\ 0 & -1 \end{pmatrix} \quad (2.7)$$

From Equation (2.6) it is possible to see a close relation between density matrices and the Bloch Sphere. In fact, the extremes of the x-, y- and z- axis of the sphere are eigenstates of their correspondent σ_x , σ_y , σ_z Pauli matrix.

The general superposition state in Equation (2.1) has the following density matrix

$$\rho = \begin{pmatrix} |\alpha|^2 & \alpha\beta^* \\ \alpha^*\beta & |\beta|^2 \end{pmatrix}. \quad (2.8)$$

Elements on the diagonal represent the probabilities $|\alpha|^2$ and $|\beta|^2$ of measuring each of the z basis states and comes from the product $|0\rangle\langle 0|$ and $|1\rangle\langle 1|$. As for the off-diagonal, they represent coherence between the terms $|0\rangle$ and $|1\rangle$, and comes from the cross product of horizontal and vertical polarization terms.

It is clear that this formalism is useful to describe quantum states and now we shall see some important properties derived from it, specifically the Purity and Fidelity of a state.

Purity

A pure state $|\psi\rangle$ is a state that cannot be written as a convex combination of other states. If one is able to make this decomposition, the state will be a mixed state, described by the density matrix ρ . The trace of the square of the density matrix sets a bound for the purity of the state:

¹The Pauli matrices σ_x , σ_y and σ_z can also be written as σ_1 , σ_2 and σ_3 , respectively.

$$\text{tr}(\rho^2) = 1, \quad \text{for pure states} \quad (2.9)$$

$$\text{tr}(\rho^2) < 1, \quad \text{for mixed states.} \quad (2.10)$$

This follows from the fact that for a pure state $|\psi\rangle$, we have $\rho = |\psi\rangle\langle\psi|$, $\rho^2 = |\psi\rangle\langle\psi|$ and then $\text{tr}(\rho^2) = \text{tr}(\rho) = 1$.

Fidelity

Fidelity is a measure of the distance between two states, ρ_1 and ρ_2 , and can be interpreted as how similar one state is to the other. It is defined as [25]

$$\mathcal{F}(\rho_1, \rho_2) = \left(\text{Tr} \sqrt{\sqrt{\rho_1} \rho_2 \sqrt{\rho_1}} \right)^2 \quad (2.11)$$

where the square root of a matrix A is a matrix B that satisfies $BB = A$. This definition is also known as Bures Fidelity. In the case one state is pure, say $\rho_1 = |\psi_1\rangle\langle\psi_1|$, we have $\mathcal{F} = |\langle\psi_1|\rho_2|\psi_1\rangle|$, and if both states are pure the fidelity will be reduced to an overlap between the states, $|\langle\psi_1|\psi_2\rangle|^2$, where $\rho_2 = |\psi_2\rangle\langle\psi_2|$. The fidelity is a symmetric function on both states and is real-valued, $0 \leq \mathcal{F}(\rho_1, \rho_2) \leq 1$. When $\mathcal{F} = 0$, ρ_1 and ρ_2 are orthogonal, and $\mathcal{F} = 1$ means $\rho_1 = \rho_2$.

2.3 Generation of entangled states

Entanglement is a global property of a system composed of two or more subsystems, such that we have knowledge about global properties (like the correlations that we shall discuss later) but little to no knowledge about the state of each subsystem. Entangled subsystems share a deep connection that cannot be described looking at each subsystem independently. A criteria used to characterize this property is the non-separability, where if a bipartite state W can be written as a convex combination of product states

$$W = \sum_i p_i \sigma_i^A \otimes \rho_i^B, \quad (2.12)$$

A and B being Alice's and Bob's subsystems, it is not entangled. On the contrary, if the state cannot be written in this manner, it is entangled. The simplest examples of non-separable states

are the Bell States ²

$$|\Phi^\pm\rangle = \frac{1}{\sqrt{2}} (|00\rangle \pm |11\rangle) \quad (2.13)$$

$$|\Psi^\pm\rangle = \frac{1}{\sqrt{2}} (|01\rangle \pm |10\rangle), \quad (2.14)$$

which are examples of maximally entangled bipartite states.

Suppose the state $|\Phi^+\rangle$ is prepared and the first qubit is sent to one party, Alice, and the second qubit is sent to Bob. Before any measurement, the state of both parties could be either $|0\rangle$ or $|1\rangle$, but if Alice performs a measurement in the $\{0/1\}$ basis she will be able to tell what state Bob will measure. If her result was $|0\rangle$, his state will be prepared in the state $|0\rangle$, and if her result was $|1\rangle$, his state will be prepared in $|1\rangle$. Bob's state can be collapsed to $|0\rangle$ or $|1\rangle$ by Alice's point of view, but for Bob, who has no knowledge of the result or perhaps even that a measurement was performed, it is still as a combination of the pure states $|0\rangle\langle 0|$ and $|1\rangle\langle 1|$, or as it is known, a statistical mixture. We can see this by writing Bob's state, ρ^B , before or after Alice's measurement, by just tracing Alice from their joint state:

$$\rho^B = \text{Tr}_A W \quad (2.15)$$

$$= {}_A\langle 0| \rho |0\rangle_A + {}_A\langle 1| \rho |1\rangle_A \quad (2.16)$$

$$= \frac{|0\rangle_B \langle 0| + |1\rangle_B \langle 1|}{2} \quad (2.17)$$

where the subscript on bra-ket notations represent the system they belong to, A for Alice and B for Bob. Thus, as Alice's measurement does not affect Bob's state there is no faster than light communication and no violation of special relativity.

The most common source of entangled photons relies on a non-linear optical process called Spontaneous Parametric Down-Conversion (SPDC) [26]. When light incides on a crystal that contains non-linear properties, it induces an electric dipole moment inside the material, which changes the dielectric polarization (\vec{P}). This dielectric polarization is related to different orders of the electric field and can be written as the following series,

$$\vec{P}(t) = \epsilon_0 \left(\chi^{(1)} \vec{E}(t) + \chi^{(2)} \vec{E}^2(t) + \chi^{(3)} \vec{E}^3(t) + \dots \right) \quad (2.18)$$

²This notations shall be used interchangeably in this dissertation: $|\psi\rangle \otimes |\phi\rangle = |\psi\phi\rangle = |\psi\rangle |\phi\rangle = |\psi, \phi\rangle$.

where ϵ_0 is the permittivity of the vacuum, $\chi^{(n)}$ is the n -th order coefficient of dielectric susceptibility and E denotes the electric field. The $\chi^{(1)}$'s are normally orders of magnitude bigger than the non-linear χ 's ($n > 1$) making their contributions typically very small. For non-linear processes to be observable, the intensity of the electric field must be high enough so that the quadratic or higher orders of E make the other terms relevant³.

For an electric field of the form $E(t) = E_0 e^{-i(kx-\omega t)} + E_0 e^{i(kx-\omega t)}$, where E_0 is the electric field amplitude, ω is the angular frequency and $k = 2\pi/\lambda$ is the wave number, the second term of the Equation (2.18), which is quadratic in the electric fields, will lead to an oscillatory term of frequency 2ω . In optics it can correspond to the conversion of a pump photon with frequency ω_p into two photons, called "twin photons", with frequencies ω_i and ω_s , where the subscript p is for pump, i for idler and s for signal. Although SPDC happens for high intensities, its efficiency is considerably low. To optimize the conversion, a condition related to the conservation of energy and momentum, generally known in non-linear optics as *phase matching*, must be satisfied. These conditions applied to the conversion of one photon into two can be written as

$$\omega_p = \omega_i + \omega_s, \quad (2.19)$$

$$\vec{k}_p \approx \vec{k}_i + \vec{k}_s. \quad (2.20)$$

From Equations (2.19) and (2.20) it is possible to see a strong correlation between the idler and signal photons concerning both energy and momentum. One interesting case is when both twin photons have the same frequency ($\omega_i = \omega_s$) and momentum, in modulus ($|\vec{k}_i| = |\vec{k}_s|$). In this situation, the emission has a rotational symmetry, forming a cone shape, as in Fig 2.2. In order to obtain these conditions, the crystal has to be cut in a way that the polarization of the incident light forms an specific angle Θ with the optical axis. For a uniaxial crystal, two types of conversion can occur, depending on Θ . Type I conversion occurs when the pump polarization is in the extraordinary (e -) plane and generates two ordinary (o -) polarized ones. The extraordinary plane is defined as being on the plane formed by the principal axis of the crystal and the wave vector of the pump photon, while ordinary axis is perpendicular to this plane. Type II down-conversion is when one e -polarized pump creates one e - and one o -polarized photon. Therefore, when the e -axis of a crystal is aligned with polarized light, it is possible to create states of the form

³In condensed matter $\chi^{(2)}$ usually is 10^{-12} times smaller than $\chi^{(1)}$. So, for the second order term to be relevant the amplitude of E must be of the order of $10^{11} V/m$ ($\chi^{(1)}E(t) \approx \chi^{(2)}E^2(t)$) [27]

$$|\psi\rangle = |HH\rangle \quad \text{or} \quad |\psi\rangle = |VV\rangle \quad [\text{Type I}] \quad (2.21)$$

$$|\psi\rangle = |HV\rangle \quad \text{or} \quad |\psi\rangle = |VH\rangle \quad [\text{Type II}] \quad (2.22)$$

Equations (2.21) and (2.22) correspond to separable states. In order to obtain entangled states from these crystals, one needs to satisfy certain conditions. Specifically for Type I, one can use two crystals under the following two conditions [26, 28]: first, they have to be orthogonally aligned between each other ($e_{-1} \perp e_{-2}$). Second, the length of both crystals must be smaller than the coherence length of the pump beam, in other words, the generation of photons in both crystals must be indistinguishable. Furthermore, the pump beam must be in a superposition state of horizontal and vertical polarizations in order to have a chance to be converted by either one of the crystals. For a pump polarized at 45° , the resulting states from this process are the Bell states $|\Phi^\pm\rangle$.

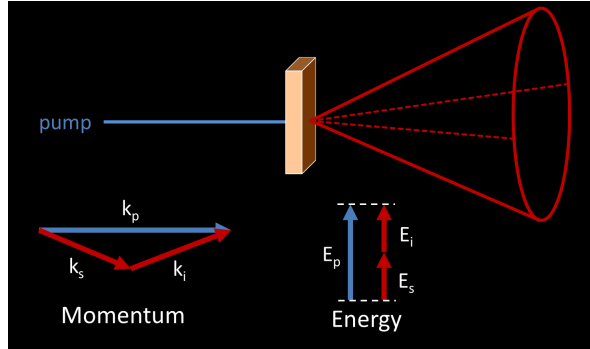


Figure 2.2: **Scheme of a Spontaneous Parametric Down-Conversion in a Type I crystal.** Due to conservation of energy and momentum, the downconverted photons are diametrically opposite and have the same polarization. At the bottom, conservation relations are illustrated.

Although polarization is one of the most known and used degrees of freedom for the generation of entanglement, there are other degrees of freedom that can be exploited as well. Let us now discuss entanglement in spatial modes. In this type of entanglement, the path of a photons is correlated with the path of its twin photon. The cone-shaped emission of Type-I crystals is an example of this and can be easily visualized. Consider the emission cone and split it in two hemispheres, up and down. Now, as a result from momentum conservation, when a photon is emitted on one hemisphere, its twin will be on the opposite hemisphere. This creates the following state

$$|\phi\rangle = \frac{1}{\sqrt{2}} (|ud\rangle + |du\rangle) \quad (2.23)$$

where $|u\rangle$ is for the upper path state and $|d\rangle$ for the lower.

Combining the entanglement on these two degrees of freedom of the same photon is possible to create a *hyper-entangled* [23, 24] state

$$|\Psi\rangle = \frac{1}{2} (|HH\rangle + |VV\rangle) \otimes (|ud\rangle + |du\rangle) \quad (2.24)$$

Hyper-entangled states were proven to be useful for a handful of applications and amongst them is quantum super-dense coding [29, 30] and quantum key distribution [31].

2.4 State operations

Quantum states can be manipulated through unitary operations, like rotations and phase shifts. Here we explore the use of wave-plates, beam splitters (PBS) and beam displacers (BD) in order to manipulate polarization and path of the photons.

2.4.1 Waveplates

Manipulation of the polarization of light can be done using birefringence. A birefringent material is optically anisotropic, meaning that different incident light polarization orientations will feel a different refractive index. By sending light into birefringent mediums the polarization can be decomposed into two coherent components. The different refractive index adds a phase to one component of the polarization due to the different optical path lengths, and when light exits the material the superposition of the components may result in a rotated polarization. Waveplates are optical devices used to rotate the polarization, and are made of a birefringent material. They are usually manufactured in a way that the fast (e -) and slow (o -) axis are parallel to the incident face and that each of these plates has a specific length - the fast axis is also known as the optical axis. Two most common types of waveplates are Half-waveplates (HWP) and Quarter-waveplates (QWP), which apply a π and a $\pi/2$ phase difference between components, respectively. Their unitary operation on the polarization can be described as

$$U_{HWP}(\theta) = \begin{pmatrix} \cos 2\theta & -\sin 2\theta \\ -\sin 2\theta & -\cos 2\theta \end{pmatrix} \quad (2.25)$$

$$U_{QWP}(\theta) = \frac{1}{\sqrt{2}} \begin{pmatrix} i - \cos 2\theta & \sin 2\theta \\ \sin 2\theta & i + \cos 2\theta \end{pmatrix} \quad (2.26)$$

where θ is the angle of the optic axis of the wave-plate with respect to the vertical axis. By careful analysis of these two operations one is able to see that combinations of waveplates allows the transformation of an initial state into any other state.

These rotations are easy to grasp by looking at the Bloch sphere (Figure 2.1), where the HWP and QWP rotate the state around the waveplate optical axis by an angle of π and $\pi/2$, respectively [32]. The waveplate optical axis is parallel to the e -axis and, on the Bloch sphere, it can be seen as on the xz -plane with θ on Equations (2.25) and (2.26) representing a rotation of 2θ on the sphere and with the position of $\theta = 0$ being the z -axis.

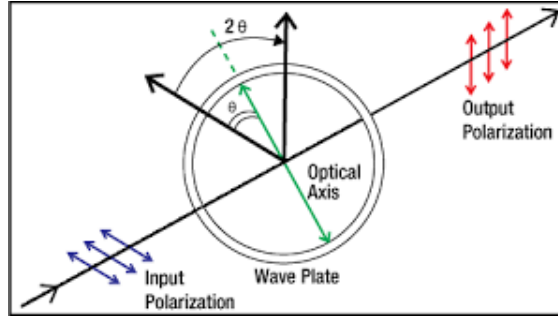


Figure 2.3: **A Half-waveplate rotating a horizontal polarization into vertical polarization.** The optical axis (green axis) is along the diagonal direction ($\theta = 45^\circ$) and the incident polarization undergoes a rotation of π around the optical axis of the HWP.

2.4.2 Beam displacer

There are several materials that possess the birefringence necessary to be used as a beam displacer (BD), but the most common are calcite crystals, probably due its natural occurrence and large birefringence. It consists of a uniaxial birefringent crystal, cut so that one polarization direction corresponds to the e -direction and the other to the o -direction. For calcite the refractive indices are:

$$n_o = 1.658$$

$$n_e = 1.486$$

Being a different medium than air, the BD adds a delay to the photons going through it compared to propagation in free space. Also, due to the birefringence, it promotes a transverse shift of the beam, an effect known as transverse “walk-off”. In other words, an incident beam with the polarization aligned to the optical axis will see a refractive index n_e , and a perpendicular polarization in reference to the optical axis will feel a different refractive index, namely n_o . This phenomena where light being transmitted through an anisotropic crystal is refracted to different angles according to its polarization is called Double Refraction (Figure 2.4). It will create a distinct path for each polarization and when they leave the crystal there will be a difference in their transverse position. The amount of displacement depends on the difference between the refractive indices and the length of the crystal, the larger it is, the larger will be the difference.

$$d = (n_e - n_o)L \quad (2.27)$$

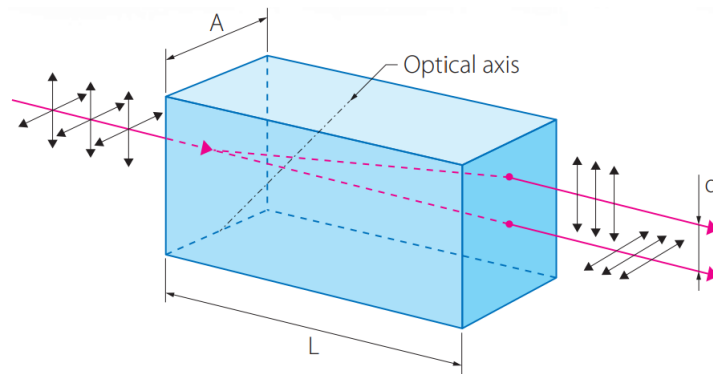


Figure 2.4: **Light with a combination of two orthogonal polarizations traversing a beam displacer.** The beam that does not have its direction changed is called *ordinary-ray* (*o-ray*) and the shifted one is called *extraordinary-ray* (*e-ray*). The indices A and L represent the dimensions of the crystal and d is the displacement between the beams. Image taken from www.altechna.com.

Beam displacers can also be used to do the inverse operation i.e., instead of separating different polarizations it can superpose them. Looking backwards at the BD it will take two different polarizations and merge them into one single beam. This can be used to convert path information

into polarization information, as we shall see in more detail later.

2.4.3 Beam splitter

A beam splitter (BS) is a glass cube with a mirror cutting it diagonally, which affects the transmission or reflectivity of light, depending on the characteristics of the mirror. The most usual type of BS is the 50/50, where the mirror reflects half of the incident light and transmits the other half. In this case the incident photon will have a 50% chance of being either reflected or transmitted, turning it into a superposition state of the output paths.

Mainly, the passage through a BS may cause a:

1. Change in phase due to the passage on the glass
2. Change in direction due to possible reflection
3. Change in phase due to the reflection and passage over the mirror

The beam direction change can be visualized as an electromagnetic field, E_a , hitting one side of a mirror and getting transmitted and reflected, E_c or E_d , respectively. Another incident electromagnetic field, E_b , could also hit the mirror on the opposite side and be transmitted and reflected, E_d or E_c , respectively (Figure 2.5).

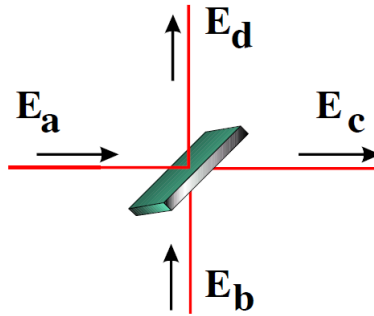


Figure 2.5: **General representation of a beam-splitter.** E_a and E_b are possible incident beams, while E_c and E_d are possible outgoing beams. Figure taken from Luiz Davidovich's lectures.

Another important type of beam splitter is the Polarizing Beam Splitter (PBS). Its mirror is made from a birefringent material, thus it is sensible to polarization and can transmit light that is horizontally polarized while reflecting the vertical polarization, or the inverse, depending on the manufacturer specifications [see Figure (2.6)]. This operation is written as

$$\begin{pmatrix} E_c \\ E_d \end{pmatrix} = \begin{pmatrix} t & -r \\ r & t \end{pmatrix} \begin{pmatrix} E_a \\ E_b \end{pmatrix} \quad (2.28)$$

where $t = \cos(\theta/2)$ is transmittance, $r = \sin(\theta/2)$ is reflectivity, θ is the angle between the polarization and the optical axis of the mirror, and they must satisfy $r^2 + t^2 = 1$. In some experiments the two spatial modes for the incident beams (E_a and E_b) are used, but in our case there will be only one ($E_a = 1$ and $E_b = 0$).

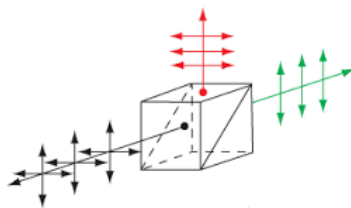


Figure 2.6: **Scheme of a PBS operation when the beam has a diagonal polarization, a combination of horizontal and vertical polarizations.** While going through the PBS the horizontal component of the beam is reflected upwards while the vertical one is transmitted. Figure taken from www.thorlabs.com

2.5 State measurement

The minimum set of orthogonal states that are sufficient to span all states in a given space is defined as an orthogonal basis. To completely determine the state of a qubit one needs to perform a set of measurements that takes into account all the states from a basis. The procedure to fully characterize the state is called *quantum state tomography* and can be done for any degree of freedom. Daniel F. V. James *et.al* [33] showed that, for polarization states, one can describe the density matrix using only four parameters. These four parameters are the so called *Stokes parameters*, described as

$$\mathcal{S}_0 \equiv \mathcal{N}(\langle H | \hat{\rho} | H \rangle + \langle V | \hat{\rho} | V \rangle) \quad (2.29)$$

$$\mathcal{S}_1 \equiv \mathcal{N}(\langle H | \hat{\rho} | H \rangle - \langle V | \hat{\rho} | V \rangle) \quad (2.30)$$

$$\mathcal{S}_2 \equiv \mathcal{N}(\langle A | \hat{\rho} | A \rangle - \langle D | \hat{\rho} | D \rangle) \quad (2.31)$$

$$\mathcal{S}_3 \equiv \mathcal{N}(\langle R | \hat{\rho} | R \rangle - \langle L | \hat{\rho} | L \rangle) \quad (2.32)$$

where each parameter corresponds to a projection measurement. S_0 is the intensity measurement, while S_1 , S_2 and S_3 are the Bloch sphere z -, x - and y -axis projections, respectively. Given the Stokes parameters, the density matrix can be reconstructed by the formula

$$\hat{\rho} = \frac{1}{2} \sum_{i=0}^3 \frac{S_i}{S_0} \hat{\sigma}_i \quad (2.33)$$

where $\hat{\sigma}_{1,2,3}$ are the Pauli matrices $\hat{\sigma}_{x,y,z}$ and σ_0 is the identity matrix. One set for the four projection measurements is $\hat{\mu}_0 = |H\rangle\langle H| + |V\rangle\langle V|$, $\hat{\mu}_1 = |H\rangle\langle H|$, $\hat{\mu}_2 = |D\rangle\langle D|$ and $\hat{\mu}_3 = |R\rangle\langle R|$. Accordingly, the case of two qubits requires a combination of these measurements for each qubit, resulting in 4^2 measurements, represented by $\hat{\mu}_i \otimes \hat{\mu}_j$ ($i, j = 0, 1, 2, 3$).

In the case of the state (2.24) two degrees of freedom are present, polarization and path. For the polarization tomography one needs a combination of a QWP and a HWP followed by a PBS and a photon detector. The waveplates are used to unitarily convert any polarization into the states $|H\rangle$ or $|V\rangle$. After that, a PBS splits the two different polarizations to distinguish between them and a single photon detector (SPD) registers the photon. For instance, if the initial state is $|D\rangle$ or $|A\rangle$, a QWP set to $\pi/4$ and a HWP to $\pi/8$ in reference to the horizontal direction, will rotate the polarization to the eigenstates of σ_z , $|H\rangle$ and $|V\rangle$, respectively. Thereafter, the PBS will separate these two polarizations, so that the original state $|D\rangle$ is transmitted and $|A\rangle$ is reflected [see Figure (2.7)]. Projection angles for each polarization measurement basis is depicted in the following table.

	QWP	HWP
σ_z	0°	0°
σ_x	$22, 5^\circ$	45°
σ_y	$22, 5^\circ$	0°

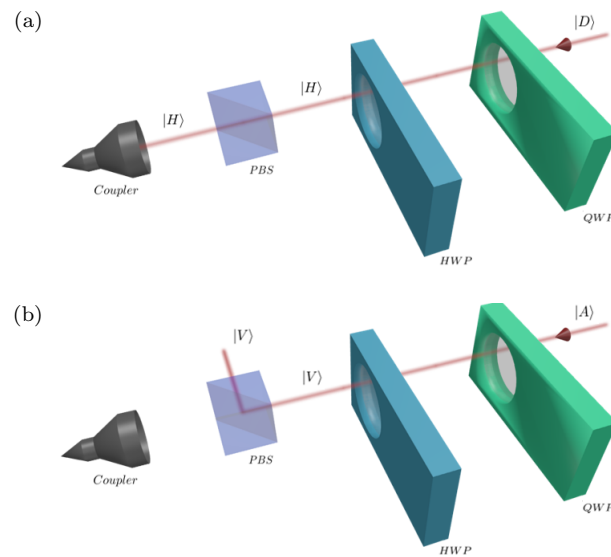


Figure 2.7: **Scheme of a polarization tomography.** (a) The incident photon is diagonally polarized and after going through the QWP and the HWP it becomes horizontally polarized. Then, after being transmitted by the PBS the photon is detected. (b) The incident photon is anti-diagonally polarized. After its passage through the waveplates it becomes vertically polarized and gets reflected at the PBS.

Path tomography will work similarly as in the case of polarization, but with the addition of two optical elements before the QWP - one is a HWP on the lower path with an angle of $\pi/4$ between the optical axis and the vertical axis, and the other is a beam displacer. These two elements perform a map from path to polarization and subsequently a regular polarization tomography takes place. As an example consider one horizontally polarized photon on one of the two paths. If the photon is on the upper path it will remain unchanged, and if it is on the downward path the HWP will change it to vertical polarization. Then, the two paths are coherently merged by the BD. The resulting state will be either a horizontal polarization state corresponding to the upper path, or a vertical polarization state corresponding to the downward path. This maps path information into polarization information [see Figure (2.8)].

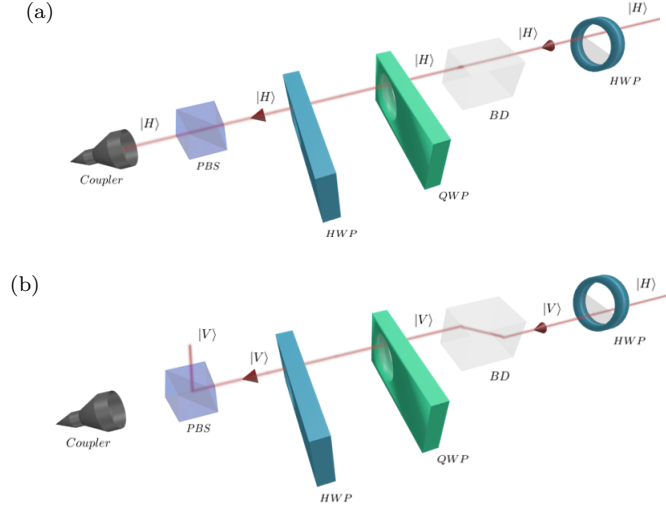


Figure 2.8: **Scheme of a photon's path discrimination.** (a) A horizontally polarized photon on the upper path suffer no action by the BD. (b) A horizontally polarized photon on the downward path is converted to vertical by the HWP, and the BD transversally shifts it to the upper path. The transversal shift on (b) move the photon to the same path as the photon from (a). In both cases, after the BD, a regular polarization tomography takes place.

2.6 State reconstruction

In general, due to experimental errors, a direct state reconstruction from the measurement results return a density matrix that does not satisfy certain physical required properties, like positivity. In order to obtain a physical density matrix, the protocol of maximum likelihood estimation is implemented [33]. This protocol can be broken down into three steps:

1. Generate an arbitrary matrix that has all mathematical requirements for a physical density matrix (positive, hermitian and normalized).

The general matrix created for a two-qubit system will have sixteen parameters and can be written as $\hat{\rho}_p(t) = \hat{T}^\dagger(t)\hat{T}(t)/\text{Tr}\{\hat{T}^\dagger(t)\hat{T}(t)\}$, where

$$\hat{T}(t) = \begin{pmatrix} t_1 & 0 & 0 & 0 \\ t_5 + it_6 & t_2 & 0 & 0 \\ t_{11} + it_{12} & t_7 + it_8 & t_3 & 0 \\ t_{15} + it_{16} & t_{13} + it_{14} & t_9 + it_{10} & t_4 \end{pmatrix} \quad (2.34)$$

2. Write the likelihood function between the generated matrix and the experimental results.

The likelihood function is a function of the 16 different tomography measurement values

n_ν ($\nu = 1, 2, \dots, 16$), whose expected value is $\bar{n}_\nu = \mathcal{N} \langle \psi_\nu | \hat{\rho} | \psi_\nu \rangle$, where $\mathcal{N} = \sum_{\nu=1}^4 n_\nu$. It is expressed as

$$\mathcal{L}(t_1, t_2, \dots, t_{16}) = \sum_{\nu=1}^{16} \frac{[\mathcal{N} \langle \psi_\nu | \hat{\rho}_p(t_1, t_2, \dots, t_{16}) | \psi_\nu \rangle - n_\nu]^2}{2\mathcal{N} \langle \psi_\nu | \hat{\rho}_p(t_1, t_2, \dots, t_{16}) | \psi_\nu \rangle} \quad (2.35)$$

3. Optimize the parameters $(t_1, t_2, \dots, t_{16})$ to find the maximum value for $\mathcal{L}(t_1, t_2, \dots, t_{16})$.

Finding the maximum value for $\mathcal{L}(t_1, t_2, \dots, t_{16})$ is the same as finding the density matrix that best describes the system measured, that is, the matrix from where the measurements most likely come from.

Chapter 3

Steering

This chapter introduces global properties shared between two subsystems, places steering amidst them, and defines a steering quantifier. Section 3.1 begins with a background on entanglement and non-locality, and defines them according to probability distributions. Later, steering is introduced in a way that is analogous to entanglement and non-locality. In Section 3.2 an operational approach is given and in Section 3.3 a quantifier for steering is reviewed. At last, in Section 3.4 is a description of the protocol used for steering distillation.

3.1 Theory

Entanglement, as previously mentioned, is a quantum correlation that arises naturally when there is a superposition state composed of two different subsystems that can only be correctly described using a quantum mechanics formalism considering both subsystems jointly. Some entangled states, such as the Bell states for example, also present a property called "Bell Non-locality", which is a correlation stronger than entanglement, in the sense that entanglement does not imply Bell non-locality, but the only physical examples of Bell non-locality in nature that we know of are entangled systems.

Quantum entanglement, or more generally, quantum correlations⁴, can be counter intuitive when considering the types of correlations that appear in classical mechanics. In 1935 Einstein, Podolsky and Rosen (EPR) found entanglement hard to accept. They questioned whether the quantum theory was complete or even correct, and proposed a way to possibly fix it [1]. Without

⁴Entanglement is not the only quantum correlation that exists. Other examples are discord, steering and Bell-nonlocality

going into detail, we simply call attention to the fact that EPR believed that a physically acceptable theory should be local and realistic. Quantum theory, they argued, is not. A local theory predicts that two spatially separated systems might have a set of past factors, described by a variable ξ , which have a causal influence on the outcome of measurements on each system. Therefore, any observed correlation would have an explanation using local variables. EPR believed that this variable ξ - known as Local Hidden Variable (LHV) - linking both systems, would explain the capacity of Alice to seemingly "affect" Bob's system.

Later, another way to solve this mystery was proposed, this time by Schrödinger, who considered quantum mechanics as incorrect only while describing non-local entangled states. In his view, the state shared between Alice and Bob would not be a superposition, the state Bob has would be a definite state even before Alice's measurement, so that Alice's influence on Bob's system would not be seen. This model became known as the Local Hidden State (LHS) model [8].

In 1964 John Stewart Bell addressed the problem of locality and realism in quantum mechanics, and started what would become a series of tests that prove the local-realistic view of the world to be incorrect. Bell derived an inequality that placed some constraints on the correlation between outcomes of measurements performed on two distant subsystems. If the results violated this inequality it meant the correlations could not be reproduced by a LHV model, therefore the state measured was not local-realistic. This is the definition of "Bell non-locality".

An operational description of Bell non-locality is the following. For a local theory, no action on a spatially separated subsystem can have any direct effect on the other, so for each value of the hidden variable, each measurement result must have an independent outcome probability. This is translated as $p(a, b|\xi) = p(a|\xi) p(b|\xi)$. In other words, a state will be non-local if and only if there exists a set of measurements within which the joint probability cannot be explained by a LHV model, i.e., if it is not the case that

$$p(a, b|x, y; \xi) = \sum_{\xi} p(a|x, \xi) p(b|y, \xi) p_{\xi}, \quad (3.1)$$

where ξ is a local hidden variable with a positive probability distribution p_{ξ} , and $p(a|x, \xi)$ and $p(b|y, \xi)$ are the local probabilities of Alice and Bob, respectively.

The description of entanglement follows a similar approach. For a state to be considered entangled it has to be non-separable, that is, it cannot be written in the form of

$$W = \sum_{\xi} p_{\xi} \sigma_{\xi}^A \otimes \rho_{\xi}^B, \quad (3.2)$$

where ξ is still a classical variable with $\sum_{\xi} p_{\xi} = 1$, and σ_{ξ}^A and ρ_{ξ}^B are local states for Alice and Bob, where σ_{ξ}^A is in Alice's hilbert space \mathcal{H}_A and ρ_{ξ}^B is in Bob's hilbert space \mathcal{H}_B .

Now consider that Alice and Bob share a quantum bipartite state and each perform a measurement on their respective subsystems. Alice (Bob) can choose a measurement x (y) according with her (his) Hilbert space \mathcal{H}_A (\mathcal{H}_B). The set of possible outcomes is $\{a\}$ and $\{b\}$ and the joint probability of obtaining the pair (a, b) conditioned to the measurements (x, y) on a system - comprising both subsystems of Alice (A) and Bob (B) - with state matrix W is $p(a, b|x, y; W)$. This probability is known as a conditional probability of obtaining $\{a\}$ and $\{b\}$, given the measurements (x, y) . In quantum mechanics, this probability can be written as

$$p(a, b|x, y; W) = \text{tr}[(\Pi_a^x \otimes \Pi_b^y) W], \quad (3.3)$$

where Π_a^x is the projector on Alice's subspace satisfying $A\Pi_a^x = a\Pi_a^x$, where A is an observable on \mathcal{H}_A and a is an eigenvalue of A . Similarly, Π_b^y is the projector on Bob's subspace and W is the system's joint state. Operationally, entanglement will be characterized when the measurements do not satisfy

$$p(a, b|x, y; W) = \sum_{\xi} p(a|x; \sigma_{\xi}) p(b|y; \rho_{\xi}) p_{\xi}, \quad (3.4)$$

where $p(a|x; \sigma_{\xi})$ and $p(b|y; \rho_{\xi})$ are conditional probabilities for Alice' and Bob's measurements on their respective subsystem.

Given entanglement and non-locality, we are able to introduce steering. It was defined by Schrödinger as being the ability of one party's choice of measurement to "conduct" the state of the other party into ensembles of different eigenstates. In one of his articles [34] he wrote: "*...by suitable measurements, take on one of the two parts only, the state (or representative or wave function) of the other part can be determined without interfering with it, but also that, in spite of this non-interference, the state arrived at depends quite decidedly on what measurements one chooses to take - not only on the results they yield.*". This inference of the state happens without real physical effects happening on the other party's system. Schrödinger did not believe it himself,

in fact, he believed a LHS model to exist. The test to check the steerability of a state also uses joint probabilities and the condition for them to be steerable is that they must not satisfy a LHS model. A state will then be considered steerable if its probability distribution cannot be written as

$$p(a, b|x, y; W) = \sum_{\xi} p(a|x, \xi) p(b|y; \rho_{\xi}) p_{\xi}. \quad (3.5)$$

This formulation is sufficient to understand the differences between steering, entanglement and non-locality, but they do not exclude one property from the other, in fact, as we shall see later, non-local states present steering and entanglement, and steerable states present entanglement, but not necessarily non-locality. There is a description for the LHS model that is operationally more useful. Consider that Bob does not measure his system, so, assuming Alice performs a measurement x and obtains the result a , Bob's state will be given by

$$\tilde{\rho}(a, x) = \sum_{\xi} p(a|x, \xi) \rho_{\xi} p_{\xi}. \quad (3.6)$$

This is the state for one outcome of the measurement “ x ”. If Bob does not know what the outcome ‘ a ’ was, he can only describe his state as an ensemble of states (3.6). Such conditional set is called an assemblage $\tilde{\rho}_{A|X} := \{\tilde{\rho}(a, x)\}$. Equation 3.6 still holds for assemblages and if it fails, that is, if there is no $p(a|x, \xi)$ that allows Bob to write his system as above, it is safe to say that the system does not obey a LHS model, therefore, it is steerable.

In review, all the knowledge needed to characterize entanglement, steering and non-locality is given by the measurement probabilities of each system. Considering Bell non-locality one notes that Equation 3.1 requires knowledge only about the measurement choice x and y , and the outcomes a and b , no knowledge about the system of Alice and Bob is necessary. For all purposes each subsystem can be considered as a black-box. As for entanglement, Equation 3.4 shows that knowledge about the measurement choice and its outcome is necessary, but, differently from Bell non-locality, the subsystem of each party has to be a quantum state. This establishes a difference between these two properties, where the conditional probabilities are given by the rules of quantum mechanics, as is the case of entanglement, or not, as is the case for Bell non-locality. Now, steering, whose presence is verified by means of Equation (3.5), is a hybrid correlation, where one of the probabilities is given by quantum mechanics, while the other is not. This description places steering as an intermediate property between entanglement and non-locality.

In 1989 R. Werner showed a hierarchy between entanglement and non-locality [3], where all non-local states are entangled, but the inverse does not hold. Later, in 2007, H. M. Wiseman *et al.* [8] widened this view by introducing steering to the hierarchy. They show that all steerable states are entangled, but not all entangled states are steerable, and also that all non-local states are steerable, but not all steerable states are non-local. Thus, steerable probability distributions are a subset of entangled ones and a superset of non-local probability distributions [see Figure (3.1)].

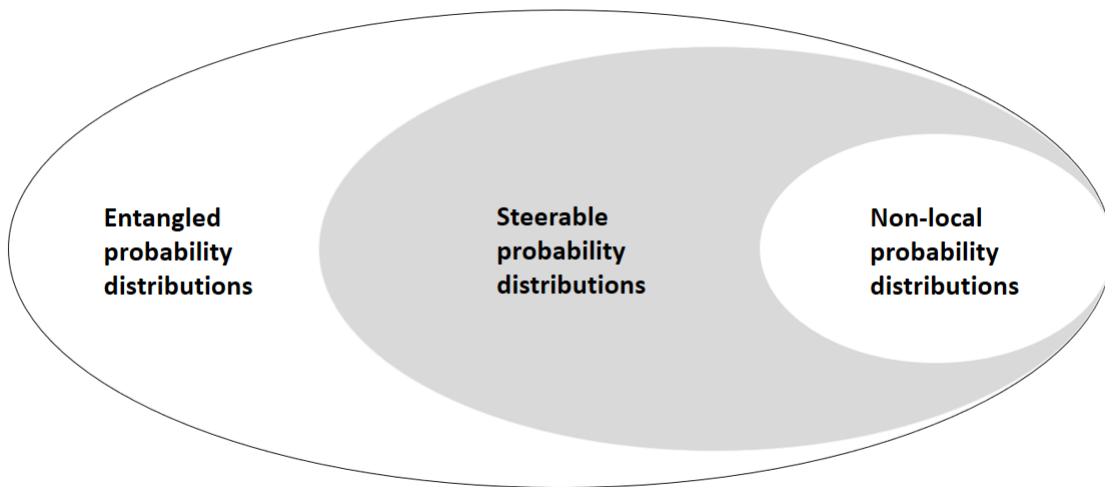


Figure 3.1: Pictorial representation of the hierarchy between entanglement, steering and non-locality.

3.2 Steering operations

A more operational approach requires a resource theory treatment. A resource theory is concerned with which ways a system can be manipulated, what transformations can be applied to this system and how to take advantage of it for some practical application. Any physical property that satisfies certain conditions can be treated as a resource, and the basic condition is that it has a class of operations, called free operations, that map a state without the resource into a state without the resource. In addition to operations, a resource theory is also concerned with the quantification of the resource, typically through some sort of measure. This measure has to be monotonic, meaning that it increases only as the quantity of the resource increases.

Essentially, a free operation does not create the resource in a system that didn't contain it in the beginning and the measurement of the system can't increase the amount of resource, only maintain or decrease it. One example of free operation for entanglement as a resource is the set of Local Operations assisted by Classical Communications (LOCC) [4]. It is composed of local

measurements by both parties and free classical communication between them. The analogous free operations for steering are the One-Way LOCC (1W-LOCC) [10]. It is also composed of local measurements, but only one of them is allowed to measure their system and communicate the result (or any other information) to the other. In the present formulation, only Bob (who has the quantum system) can measure and send information to Alice while the contrary is not allowed.

An alternative way of representing steerable states, that is useful to define 1W-LOCC's, is

$$\tilde{\rho}(a, x) := \sum_a p(a|x) |a\rangle \langle a| \otimes \rho(a, x), \quad (3.7)$$

with $\{|a\rangle\}$ being an orthonormal basis of an extended Hilbert space \mathcal{H}_E of the same dimension as \mathcal{H}_A and $\rho \in \mathcal{H}_B$. It is an abstract state representing the outcomes of Alice and not her system. $p(a|x)$ and $\rho(a, x)$ no longer depend on ξ , since it is a steerable state. Here we restrict $\rho(a, x)$ to the no-signaling assemblages, that is

$$\sum_a \rho(a, x) = \sum_a \rho(a, x') \quad \forall x, x'. \quad (3.8)$$

The definition of a 1W-LOCC is a map \mathcal{M} that takes the assemblage $\tilde{\rho}_{A|X}$ into a final assemblage

$$\tilde{\rho}_{A_f|X_f} := \mathcal{M}(\tilde{\rho}_{A|X}) = \sum_{\omega} \mathcal{M}_{\omega}(\tilde{\rho}_{A|X}) := \sum_{\omega} (\mathbf{1} \otimes K_{\omega}) \mathcal{W}_{\omega}(\tilde{\rho}_{A|X}) ((\mathbf{1} \otimes K_{\omega}^{\dagger}), \quad (3.9)$$

where K_{ω} is a map that takes \mathcal{H}_B to a final Hilbert space \mathcal{H}_{B_f} , of dimension d_f , and here it represents the measurement operator corresponding to the ω -th measurement outcome. $\mathcal{W}_{\omega}(\tilde{\rho}_{A|X})$ is defined as

$$[\mathcal{W}_{\omega}(\tilde{\rho}_{A|X})](x_f) := \sum_{a_f, a, x} p(x|x_f, \omega) p(a_f|a, x, \omega, x_f) (|a_f\rangle \langle a_f| \otimes \mathbf{1}) \tilde{\rho}(a, x) (|a\rangle \langle a_f| \otimes \mathbf{1}), \quad (3.10)$$

where it represents a map of Alice's choice of measurement x and the corresponding outcome a , based on the communication ω she received from Bob after his operation (Figure 3.2). Note that it does not take into account Alice's state or $p(a|x)$, maintaining a black-box view on Alice's side.

The process to implement \mathcal{M} is as follows: First, Bob applies an operation \mathcal{M}_{ω} on his system, with probability $p_{\Omega}(\omega)$. After this he communicates ω to Alice, being ω not an input or output,

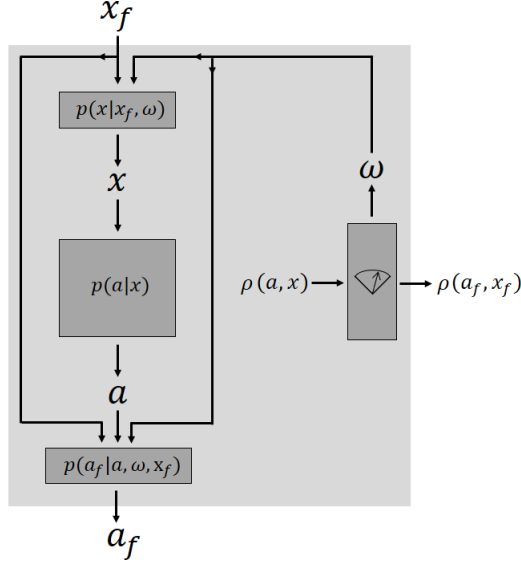


Figure 3.2: **Schematic view of a 1W-LOCC.** The initial assemblage $\tilde{\rho}_{A|X}$ consists of a quantum subsystem in one of the states $\{\rho(a, x)\}$, in Bob's possession, and a black-box with inputs x and outputs a , governed by a probability distribution $p(a|x)$, on Alice's possession. The final assemblage $\tilde{\rho}_{A_f|X_f}$ consists of a black-box with inputs x_f and outputs a_f for Alice, and an output ω with final subsystem in the state $\rho(a_f, x_f)$ for Bob. This image is an adaptation from [10].

but a tag of which operation was applied. Then, Alice generates x , with probability $p(x|x_f, \omega)$, by processing x_f and ω . She uses x as input on her initial device and gets a . At last, Alice take a , x_f and ω as inputs to a final device to generate a_f with probability $p(a_f|a, x_f, \omega)$.

3.3 Steering quantifier

Another important ingredient in a resource theory is a quantifier of the resource. Among the few proposed steering quantifiers [10, 11], we use Steering Robustness [12]. Steering Robustness is defined as the minimal amount of noise applied to the system that takes a steerable assemblage to one described by a LHS model [35]. The value obtained for robustness will quantify how steerable the state is, where the higher the value, the more steering the state has. Its formulation is similar to entanglement robustness [5], and can be defined as [35]

$$SR^{\mathcal{N}}(\tilde{\rho}_{A|X}) = \min_{\{\pi_{A|X}\}, \{\hat{\rho}_\lambda\}, t} t \quad (3.11)$$

$$s.t. \quad \frac{\tilde{\rho}_{A|X} + t\pi_{A|X}}{t+1} = \tilde{\rho}_{A|X}^{LHS} \quad \forall a, x, \quad (3.12)$$

$$\tilde{\rho}_{A|X}^{LHS} = \sum_{\lambda} D(a|x, \lambda) \rho_{\lambda} \quad \forall a, x, \quad (3.13)$$

$$\pi_{a|x} \in \mathcal{N}, \quad \rho_{\lambda} \geq 0 \quad \forall \lambda, \quad (3.14)$$

where \mathcal{N} is a set of assemblages characterised by positive semi-definite (PSD) constraints and linear matrix inequalities (LMIs). It will determine the minimum amount of a specific type of noise $\pi_{a|x}$ added to the system $\tilde{\rho}_{A|X}$, so that the final assemblage can be described by a LHS model ($\tilde{\rho}_{A|X}^{LHS}$). The weight of the system is $1/(t+1)$, while the weight of the noise is $t/(t+1)$. Equation (3.14) is derived from Equation (3.6), where it was rewritten according to a deterministic response function $D(a|x, \xi)$, using $p(a|x, \xi) = \sum_{\lambda} p(\lambda|\xi) D(a|x, \lambda)$ and $\rho_{\lambda} := \sum_{\xi} p_{\xi} p(\lambda|\xi) \rho_{\xi}$. The particular case where $t = 0$, means $SR^{\mathcal{N}}(\tilde{\rho}_{A|X}) = 0$ and the assemblage is already unsteerable.

The above formulation of steering robustness is intuitive, but there is a more practical extension of it using semidefinite programming (SDP) that says

$$SR(\tilde{\rho}_{A|X}) = \max_{\{F_{a|x}\}} \sum_{a,x} \text{tr}(F_{a|x} \tilde{\rho}_{A|X}) - 1 \quad (3.15)$$

$$subject\ to \quad \sum_{a,x} D(a|x, \lambda) F_{a|x} \leq \mathbf{1} \quad \forall \lambda \quad (3.16)$$

$$F_{a|x} \geq 0 \quad \forall a, x, \quad (3.17)$$

with $F_{a|x}$ being a hermitian matrix. The values for $\tilde{\rho}_{A|X}$ and $D(a|x, \lambda)$ are obtained through measurements, while the varying term used to optimize the above function is $F_{a|x}$. The above SDP thus provides an efficient way to calculate the SR using well-known numerical optimization techniques.

If the amount of noise necessary to make the original assemblage be described by a LHS is zero, $SR(\tilde{\rho}_{A|X})$ will be either zero or negative, meaning that the assemblage was already non-steerable. On the other hand, if any addition of noise is needed, the assemblage was steerable.

3.4 Steering distillation

Distillation is a process in which one is able to use the allowed free-operations to probabilistically increase the amount of a given resource. The process of distilling a state is already known for entanglement [22, 36–38], and at least one of these schemes resembles the approach used here for steering distillation. For entanglement, the goal is to begin with N quantum states with arbitrary entanglement and end up with a number M ($\leq N$) of quantum states, which are maximally entangled, using a set of measurement operators K such that:

$$|\psi\rangle = \alpha |00\rangle + \sqrt{1 - \alpha^2} |11\rangle \rightarrow \begin{cases} K_0 : |\psi\rangle \rightarrow |00\rangle \\ K_1 : |\psi\rangle \rightarrow \frac{|00\rangle + |11\rangle}{\sqrt{2}} \end{cases} \quad (3.18)$$

Here a local operation is performed on one of the qubits, with two possible outcomes. The operation K_0 returns a product state, while the operation K_1 gives a maximally entangled state. The Charles H. Bennett *et al.* [37] proposal for entanglement purification follows this scheme. In his proposal the measurements are local, in the sense that each party operates on their pair of qubits, and a two-way classical communication is necessary to complete the purification process. This characterises a Local Operation with Classical Communication (LOCC), one of the allowed free operations for entanglement.

The difference between entanglement and steering distillation is in the allowed free operations. For steering, we take an assemblage with a certain value of robustness and apply the 1W-LOCC with the goal of increasing steering. Experimentally, we can characterize the protocol by performing state tomography before and after a filtering operation. The result, if there was any distillation, will show that $SR_{final} \geq SR_{initial}$.

The process of distillation follows Figure 3.3. Two copies of a quantum state are generated. In our experiment, the qubit of one copy is encoded in the polarization degree of freedom, while the other is encoded in the path degree of freedom, as in Equation (2.24). Alice and Bob receive their part of the state and Bob applies a local filtering operation, as described in Equation (3.18), on his path qubit. One of the outcomes ($\omega = 0$) will eliminate the steering in the copy related to path, indicating failure of distillation of the path information, leaving the state only with information on polarization, but without any distillation. The second option ($\omega = 1$) filters the path information towards a more steerable state, and in this case we discard the polarization information. This process always results in a correlated state, where K_1 returns a distilled state.

According to the outcome of the filtering operation, different measurements are then performed by Bob to characterise his state. If the filtering resulted in a state with polarization information (K_0), polarization measurements are performed, or, if the filtering operation was K_1 , momentum measurements are performed. Then Bob communicates to Alice which operation was indeed applied. With that she will know if her system underwent the a_0 or a_1 pathway depending on ω , where if it went through a_1 the state has a higher steering robustness than the original. In this manner, we know everything about Bob's system, what was his input y - namely his choice of measurement, the operation applied K_ω and his output b - the result of his operations, giving a description of a white-box. Meanwhile, the knowledge about Alice's side is her input x and output a , and no information about what operations she might have applied, characterising her side as a black-box. This provides the necessary information to reconstruct Bob's state and Alice's statistics and recover the assemblage $\tilde{\rho}_{A|X}$.

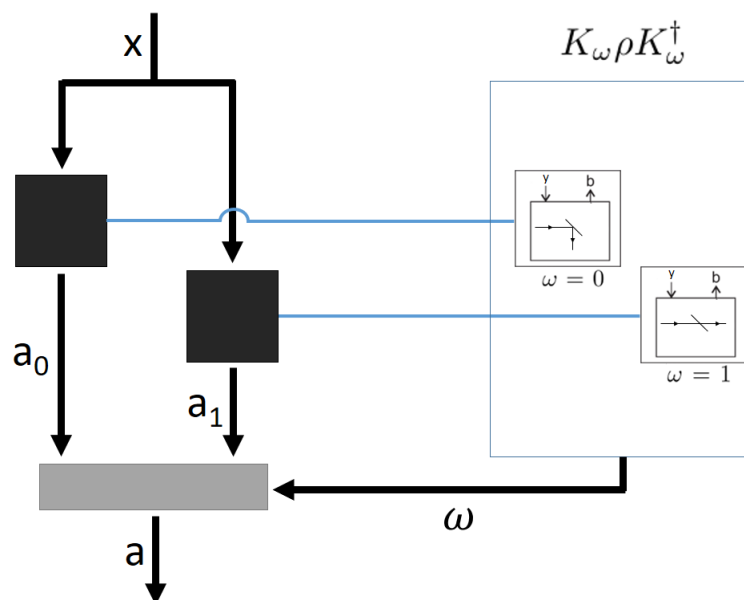


Figure 3.3: Scheme of the 1W-LOCC applied on the experiment. Black-boxes correspond to Alice's side, while white-boxes to Bob. The blue link between boxes represent correlated states shared between both parties. Here Bob can perform two different local operations, each will correspond to a different response on the black-box. The communication by Bob will let Alice know which response (a_0 or a_1) was triggered and give her an outcome a .

$$\Pi_j \tag{3.19}$$

$$j \tag{3.20}$$

Chapter 4

The experiment

In this chapter there is a description on how the experiment was implemented, with details on all equipment used (Section 4.1). In the second part of the chapter the data analysis and results are presented (Section 4.2).

4.1 Experimental implementation

The protocol described in Section 3.4 was performed using photons polarization and path degrees of freedom. The experiment begins with a He-Cd laser, used as a pump beam for SPDC (see Section 2.3), and with wavelength of 325nm. The polarization of the pump beam can be manipulated to any direction by using a combination of one HWP and one QWP. Then, a BBO crystal is used to produce pairs of photons each with half the energy of a pump photon (and wavelength doubled, 650nm). We use two Type-I BBO crystals with their optic axis perpendicularly aligned [28]. The angle of the crystals were properly aligned to yield concentric cones of SPDC pairs. In order to have a parallel circular ring beam, instead of a divergent cone, a plano-convex lens is placed in front of the BBO crystal at a distance equal to the focal length of the lens, turning the cone into a cylinder. Next, a mask selects four positions on the cylinder, containing two pairs of correlated photons (see Figure 4.1). When we start with an arbitrary polarization state of the pump beam described as

$$|\psi_1\rangle = \alpha |V\rangle + \beta |H\rangle, \quad (4.1)$$

the two-photon polarization state after the BBO crystals becomes

$$|\psi_2\rangle = \alpha |HH\rangle + \beta |VV\rangle. \quad (4.2)$$

The two-photon polarization state around the entire ring of the emission cone is given by Equation (4.2), so that using the mask selection technique we are able to prepare two pairs of entangled qubits, encoded in a single pair of photons:

$$|\psi_3\rangle = (\alpha |HH\rangle + \beta |VV\rangle) \otimes (\gamma |ud\rangle + \delta |du\rangle). \quad (4.3)$$

where $|u\rangle$ and $|d\rangle$ refer to up and down paths selected by the mask aperture. We note that the transverse momentum entanglement was used to produce the second set of entangled qubits, as discussed in Chapter 2.3. The last optical element in the preparation set is a partially reflective mirror, placed in only one path and acting only in one of the qubits, used to adjust the coefficients γ and δ to be equal to α and β .

The next step is to separate the photons between Alice and Bob. The left modes, u and d , go to Bob and the right ones go to Alice. In this way, each of them will be in possession of half of each of the entangled states in Equation (4.3).

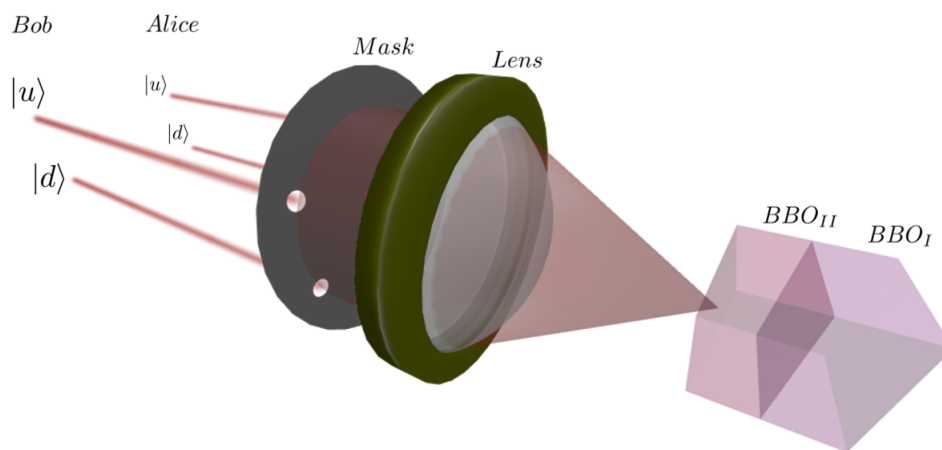


Figure 4.1: **Illustration of the cone-shaped generation of correlated photons.** The converted photons at the BBO form a cone shape emission and are transformed from a cone to a cylinder by a lens. After it a mask selects four specific positions for the photons.

Following the distillation protocol presented in the last chapter, Bob performs a local filtering

operation, which is done by a mirror with a variable transmission coefficient positioned only on his down path ($|ud\rangle$). The mirror is actually a variable attenuation filter that happens to be reflective (Thorlabs NDL-25C-4), so that it contains a linear gradient of reflectivity along its length, at one edge it reflects 100% of the incoming light ($R = 1$) and at the other it transmits 100% ($R = 0$). Placing this mirror in only the d path of photon 2 changes the ratio between γ and δ by filtering the down path amplitude (γ) to a new value (γ'), such that $\gamma' \leq \gamma$. This filtering transforms the state $|\psi_3\rangle$ into

$$|\psi_4\rangle = (\alpha |HH\rangle + \beta |VV\rangle) \otimes (\gamma' |ud\rangle + \delta' |du\rangle)$$

or

$$|\psi_4\rangle = \alpha\gamma' |HH\rangle |ud\rangle + \alpha\delta' |HH\rangle |du\rangle + \beta\gamma' |VV\rangle |ud\rangle + \beta\delta' |VV\rangle |du\rangle, \quad (4.4)$$

where we changed δ to δ' to allow for normalization. This is the state that is transmitted through the variable mirror. Note that it still contains both momentum and polarization entanglement. Meanwhile, the state that is reflected from the variable mirror will collapse the momentum entanglement to the down path. Thus, it is given by:

$$|\psi_5\rangle = (\alpha |HH\rangle + \beta |VV\rangle) |ud\rangle. \quad (4.5)$$

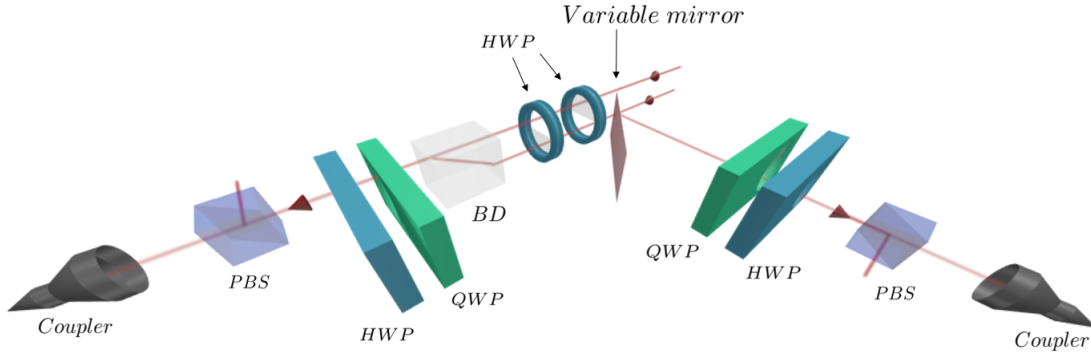


Figure 4.2: **Bob's setup.** If the photon is reflected by the variable mirror (in path $|d\rangle$), the momentum state is discarded, and polarization entanglement remains. Polarization tomography is then performed. If the photon passes through the variable mirror stage, local filtering on the momentum state was successful, and momentum tomography is performed.

After the local filtering operation, Bob will detect his photon on one of the sides of the variable mirror, reflected or transmitted. In our experiment Bob determines the side the photon went by

detecting, in the end, in one of the two detection systems. Thus, we use a type of post-selection. However, in principle, a nondemolition measurement could be performed to determine the side of the photon, without destroying it [39]. When the photon is reflected from the mirror, the local filtering operation was not successful ($\omega = 0$), meaning that the momentum state is no longer entangled. In this case, we discard the momentum state and use the polarization state of the photon pair. Polarization measurement is then performed by Bob using a set of waveplates and a PBS, and a tomography is obtained by repeating this many times for different polarization projections. On the other hand, if the photon is not reflected from the variable mirror, the local filtering procedure was successful ($\omega = 1$), and the momentum state, now with increased steering, is used by Alice and Bob. To verify the increase in steering, the photons are measured in the path degree of freedom, using a set of waveplates, a beam-displacer and the PBS. In contrast to the experimental simplicity of polarization tomography, path tomography requires the coherent recombination of the spatial modes $|u\rangle$ and $|d\rangle$, which is considerably more demanding. A simple way to do this is by a transformation of path information into polarization information, so that only simple projective polarization measurements need to be performed to measure the momentum state. This will be described in detail below in the context of Alice's system, where the transformation is similar to Bob's.

In principle, Alice waits for Bob to reveal whether the local filtering was successful or not. In our proof of principle experiment, Alice does not wait for Bob to communicate ω , instead, she tomographs her states right away. In order to do so, the two sets of tomography, path and polarization, are mounted together (see Figure 4.3). Whenever she wants to perform a path tomography the polarization waveplates are set to 0° and only the path ones are used. When the tomography is performed on polarization, she does the opposite, path waveplates stay at 0° and polarization waveplates rotate.

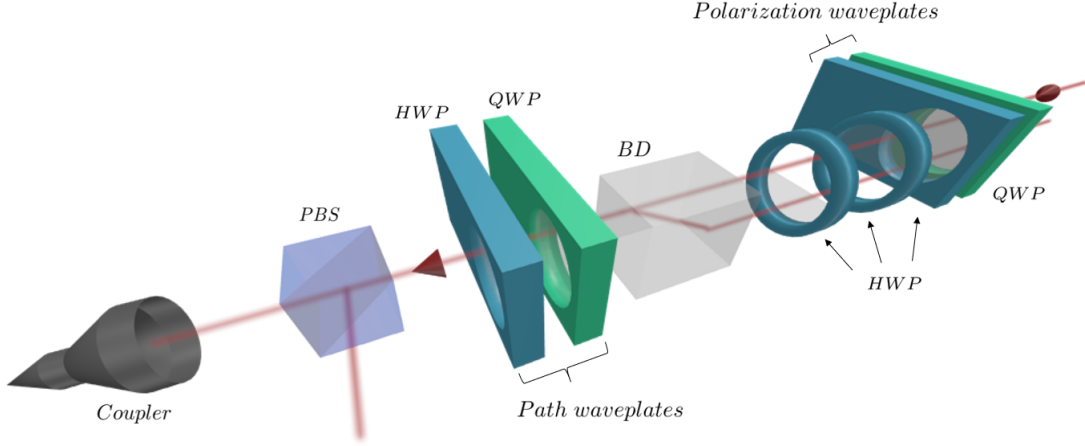


Figure 4.3: **Alice's side containing polarization and path tomography together.** At first are two waveplates responsible for polarization projection. Later is a set of two fixed waveplates, a BD and two other waveplates, which altogether form the setup for path tomography. To end the tomography setup is a PBS and a fibre coupler, which is responsible for guiding the photons to a Single Photon Detector.

Let us explain the momentum tomography in more detail. The state after the fixed waveplates, but before the beam displacer (see Figs. 4.2 and 4.3) is

$$|\psi_6\rangle = \alpha\gamma\iota|HV\rangle|ud\rangle + \alpha\delta\iota|VH\rangle|du\rangle + \beta\gamma\iota|VH\rangle|ud\rangle + \beta\delta\iota|HV\rangle|du\rangle \quad (4.6)$$

And after the beam displacer the state effectively becomes

$$|\psi_7\rangle = \alpha\gamma\iota|HV\rangle|ud\rangle + \alpha\delta\iota|VH\rangle|du\rangle \quad (4.7)$$

note that we used the equality sign, but the state is not normalized any more. Here we discarded the polarization $|H\rangle$ related to path $|d\rangle$ and polarization $|V\rangle$ related to path $|u\rangle$. When these photons exit the beam displacer they are not aligned on the path that leads to the fiber coupler, therefore they will not be detected. Also, the $|d\rangle$ photons that are vertically polarized will be shifted up, merging with the upper path. This is translated as a transformation of path $|d\rangle$ to $|u\rangle$ when the polarization on Bob is $|V\rangle$. Therefore, the State (4.7) is actually transformed to

$$|\psi_8\rangle = (\alpha\gamma\iota|HV\rangle + \alpha\delta\iota|VH\rangle)|uu\rangle. \quad (4.8)$$

We can put α in evidence and get

$$|\psi_9\rangle = (\gamma'|HV\rangle + \delta'|VH\rangle) \otimes \alpha|uu\rangle. \quad (4.9)$$

This state represents the final step into transforming momentum information to polarization information, so that polarization projective measurements can be performed to tomograph the state.

The combination of up and down path by a beam displacer must be coherent, however, the difference in refractive indices for each path and the size of the crystal are enough to destroy their coherence. For our photons at 650nm with 10nm bandwidth interference filters, the longitudinal coherence length is about $28\ \mu\text{m}$. Meanwhile, the birefringence of the beam displacers results in a path length difference of about $1.3\ \text{mm}$. To correct this, a series of glass slides are introduced on both sides of the experiment to compensate the longitudinal walk-off. The optical elements had to be carefully adjusted, but, even so, there was still an added mechanical instability factor causing this interference to oscillate. The time frame of this stability was approximately equal to the full tomography duration ($\tilde{15}$ minutes).

For a detection to occur, the photons must couple into an optical fiber, which will lead them to a Single Photon Detector (SPD). The two-photon (Alice's and Bob's) events must be in coincidence. A coincidence consists of a detection on both sides (A and B) with a specific difference in time between them. When there is a detection on any side a trigger is activated, opening a time window to have a detection on the other side. For example, if Alice detects one photon, the time window will open for Bob to detect a photon on one of his arms. If Bob has any detection inside this window means that his and Alice's photons are most likely correlated, being emitted together from the SPDC source. Otherwise, if the detection delay time is longer than the time window, we cannot trust the photons to be correlated, because the second one may have come from any other emission, therefore this event is not taken into account. The inverse case, when Bob's detection is the first, is also used to count coincidences. This coincidence detection is thus performed so that it is highly probable that every photon detected by Alice is the one correlated to the photon detected on Bob, or vice versa. The time trigger to open the detection time window was implemented by a Field-Programmable Gate Array (FPGA) programmed with LabVIEW, and the time window was set to 5 nanoseconds (ns).

Every measurement performed is composed of 10 seconds of continuous coincidence detections. This gives approximately $10\ \text{seconds}/5\ \text{nanoseconds} = 2 \times 10^9$ possible coincidence counts for a single measurement, but, in reality, we had count rates of about 2×10^2 coincidences/second, due to the finite intensity of our pump laser, as well as the spatial and spectral filtering required

to produce the hyper-entangled states. Sixteen projective measurements compose a two-qubit tomography, which is performed twice in a row so that any error, such as incorrect rotation of automated waveplates, can be identified and discarded.

All measurements can be grouped into the polarization or the path tomography. The polarization tomography alone is of a state without any filtering operations applied on it, therefore it is used to obtain information about the initial state. During the experiment, we aimed to prepare four different initial states ($|\psi_1\rangle$) considering the difference between α and β . The parameter used to characterise the state is the Population Difference (PD), where $PD = |\alpha|^2 - |\beta|^2$. All of these states have a degree of steerability and are used as reference to check for steering distillation. Photons detected while performing path tomography are those which were successfully filtered by Bob, and theoretically should have an increased steering robustness when compared with the initial state.

Summarizing, the complete setup of the experiment is shown in Figure 4.4 and a table containing all equipment used is in Appendix B.

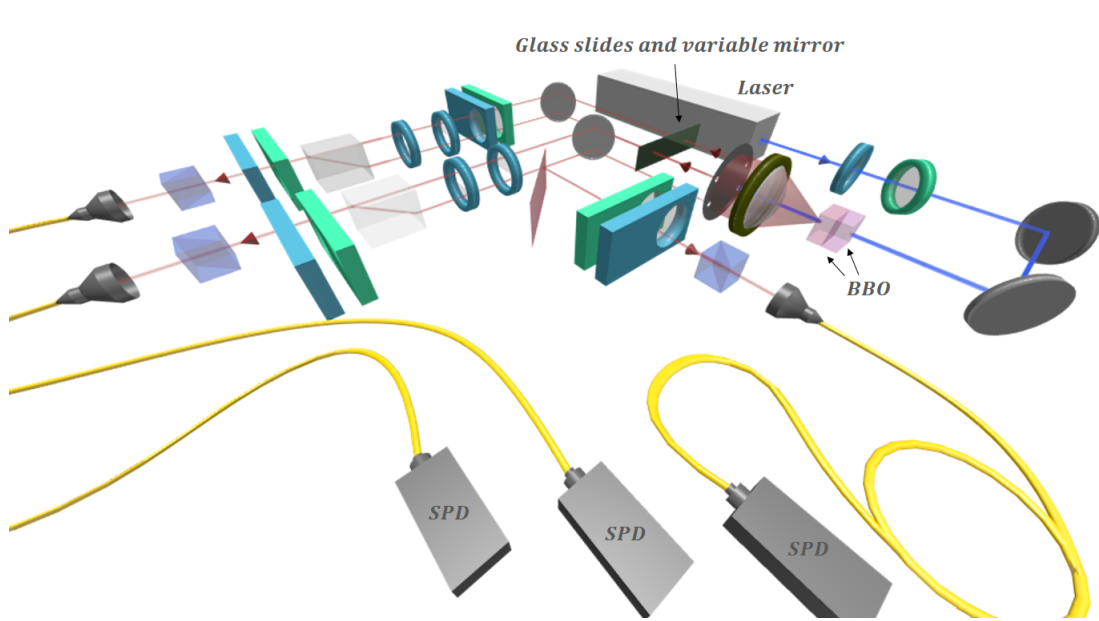


Figure 4.4: **The complete scheme used to prove steering distillation.** At the beginning, emitting the blue laser, is the laser source, followed by two waveplates and the BBO crystals, which were made bigger here for illustration. Further along is the plano-convex lens, the mask, the upper path glass slides and variable mirror, where the later is the one responsible for filtering the state to make $\alpha = \gamma$ and $\beta = \delta$. After it the photons are divided into Alice's setup and Bob's setup. There are two different mounts for waveplates, the ones represented by circular supports are movable by hand, while the ones on rectangular supports are automated waveplates.

4.2 Data processing and analysis

Using the statistics from the measurements, we obtained the initial population difference for all four cases, they were

PD path unfiltered	PD Polarization
0.20 ± 0.03	0.22 ± 0.03
0.38 ± 0.03	0.51 ± 0.03
0.59 ± 0.02	0.60 ± 0.03
0.80 ± 0.01	0.77 ± 0.02

Here we see that the two copies can be considered equal at the beginning, with a small discrepancy in one of the cases. This discrepancy does not invalidate our analysis, since the copies being different only mean that in a real procedure the distillation would not bring a big advantage. But, for the purpose of this dissertation, it will make no difference.

Further, we analysed the fidelity between the two original copies to certify that we had two identical copies at the beginning, before any local operation was applied. The values obtained for these fidelities were between 90% and 95%, confirming that we prepared two very similar copies. In addition, we reconstructed the states density matrices using the method of maximum likelihood estimation described in Section 2.6. The result for all four cases are presented in Figures 4.5 - 4.8.

Visual inspection of the density matrices shows that the resulting momentum state is more or less as expected, with coherence between the $|ud\rangle$ and $|du\rangle$ states. In most cases these coherences are real and positive. We notice in our results that for a PD of 0.6042 the coherences change phase, most likely due to a phase fluctuation between the calibration and measurement acquisition.

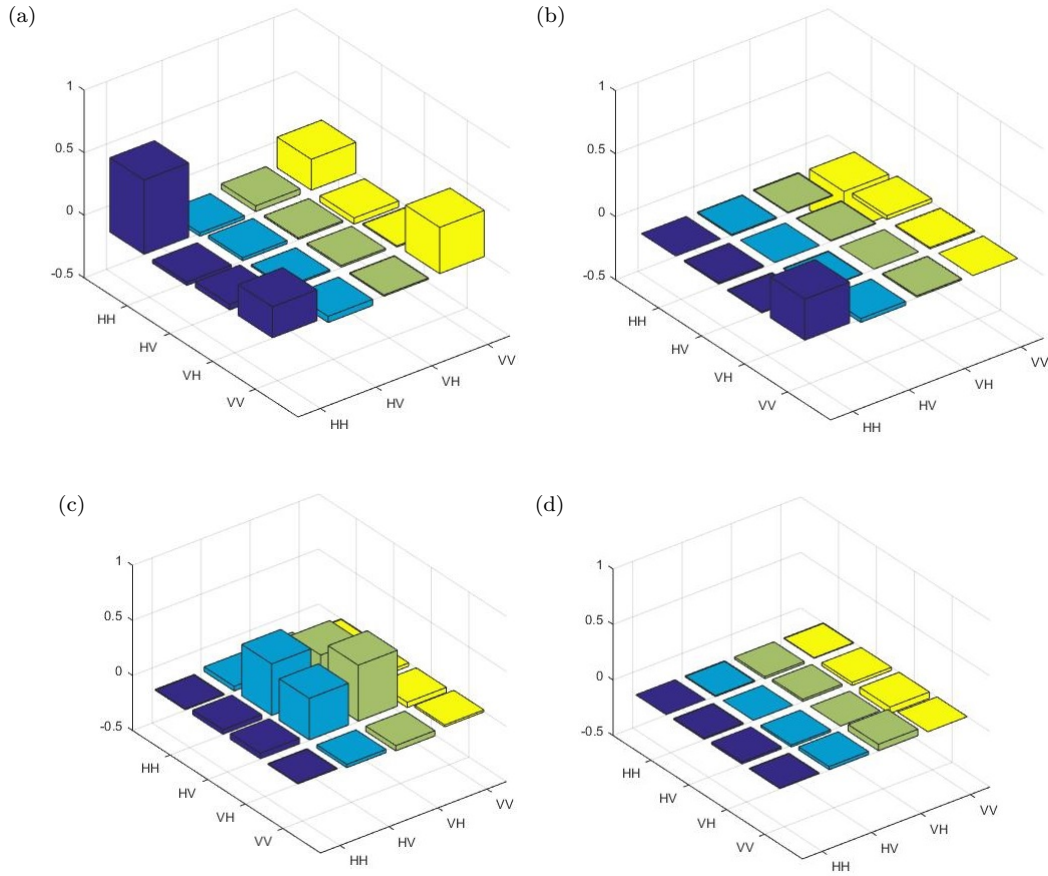


Figure 4.5: **Density matrices for the population difference of 0.2156.** 4.5a and 4.5b are the real and imaginary parts of the polarization tomography, respectively, that is, before any operation is applied. 4.5c and 4.5d are the real and imaginary part of the momentum state, respectively, after the filtering. In this two later cases path information was transformed into polarization information, therefore polarization H means path u and polarization V means path d . The path and polarization matrices present data on different spots because in polarization the correlation is between qubits with the same information on both sides ($|HH\rangle$ or $|VV\rangle$), while in path the correlation is between qubits with different information in each side ($|ud\rangle$ or $|du\rangle$)

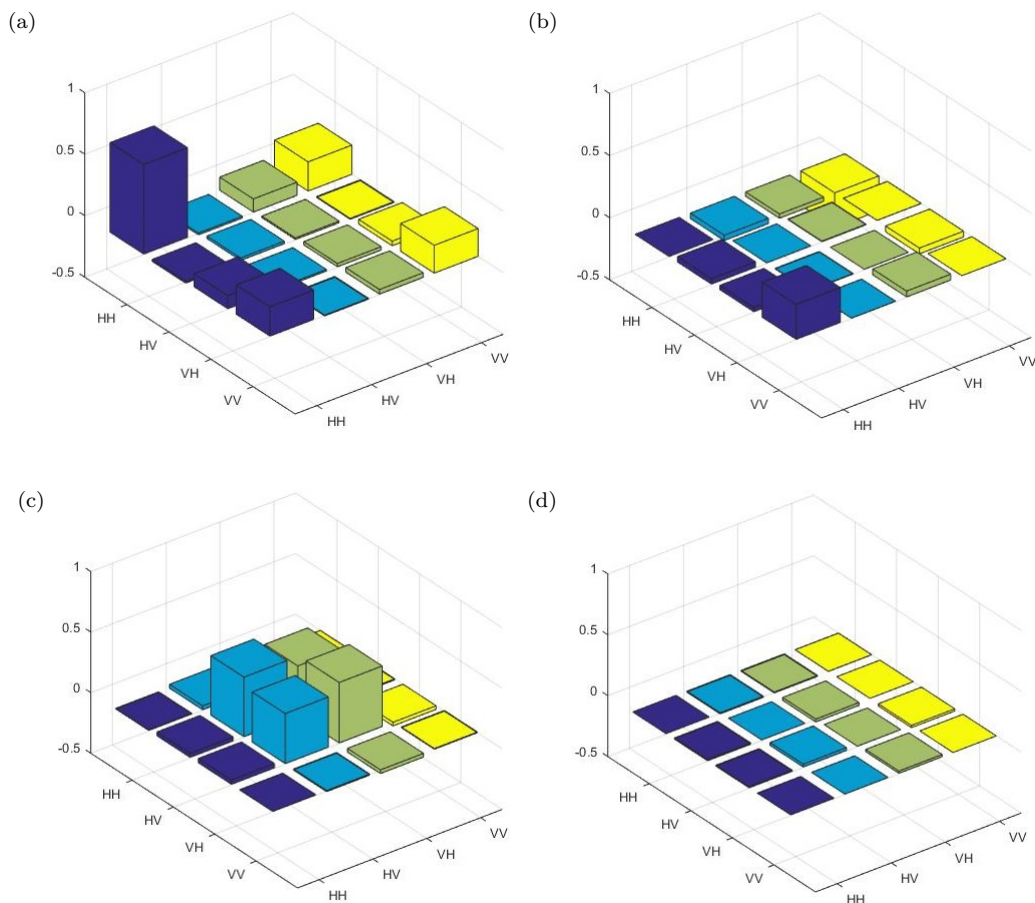


Figure 4.6: **Density matrices for the population difference of 0.5079.** 4.6a and 4.6b are the real and imaginary parts of the polarization tomography, respectively, that is, before any operation is applied. 4.6c and 4.6d are the real and imaginary part of the momentum state, respectively, after the filtering. In this two later cases path information was transformed into polarization information, therefore polarization H means path u and polarization V means path d . The path and polarization matrices present data on different spots because in polarization the correlation is between qubits with the same information on both sides ($|HH\rangle$ or $|VV\rangle$), while in path the correlation is between qubits with different information in each side ($|ud\rangle$ or $|du\rangle$)

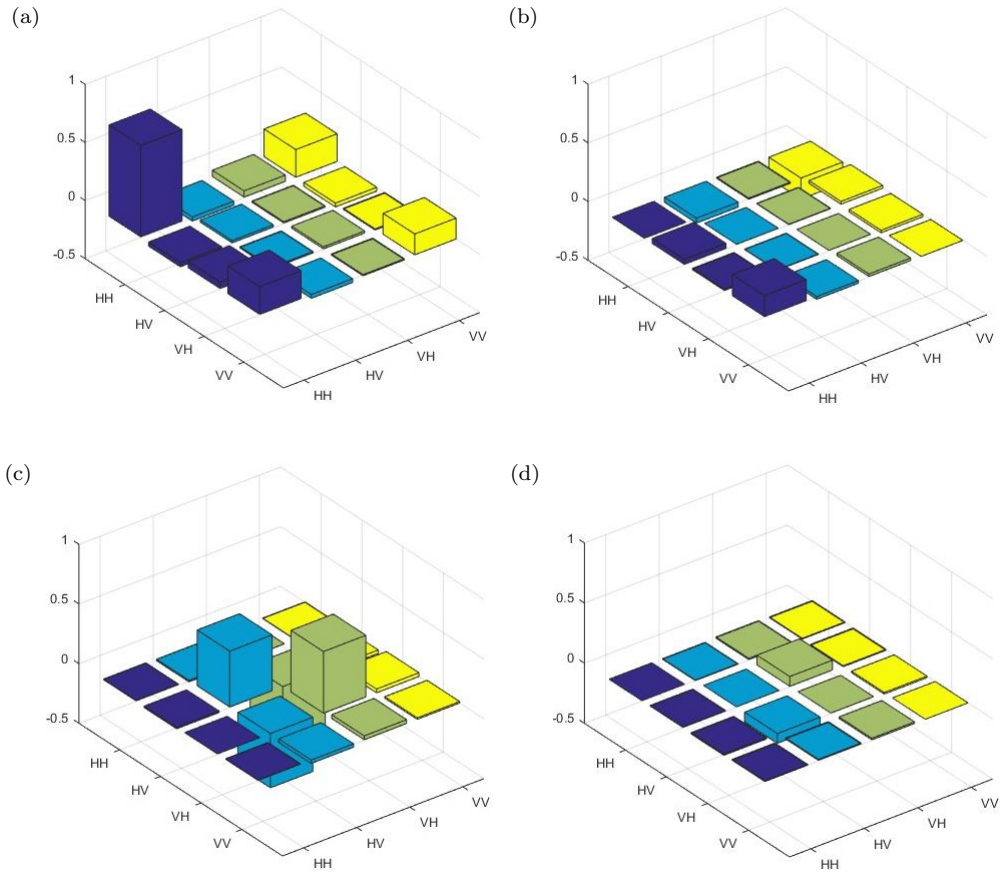


Figure 4.7: **Density matrices for the population difference of 0.6042.** 4.7a and 4.7b are the real and imaginary parts of the polarization tomography, respectively, that is, before any operation is applied. 4.7c and 4.7d are the real and imaginary part of the momentum state, respectively, after the filtering. In this two later cases path information was transformed into polarization information, therefore polarization H means path u and polarization V means path d . The path and polarization matrices present data on different spots because in polarization the correlation is between qubits with the same information on both sides ($|HH\rangle$ or $|VV\rangle$), while in path the correlation is between qubits with different information in each side ($|ud\rangle$ or $|du\rangle$)

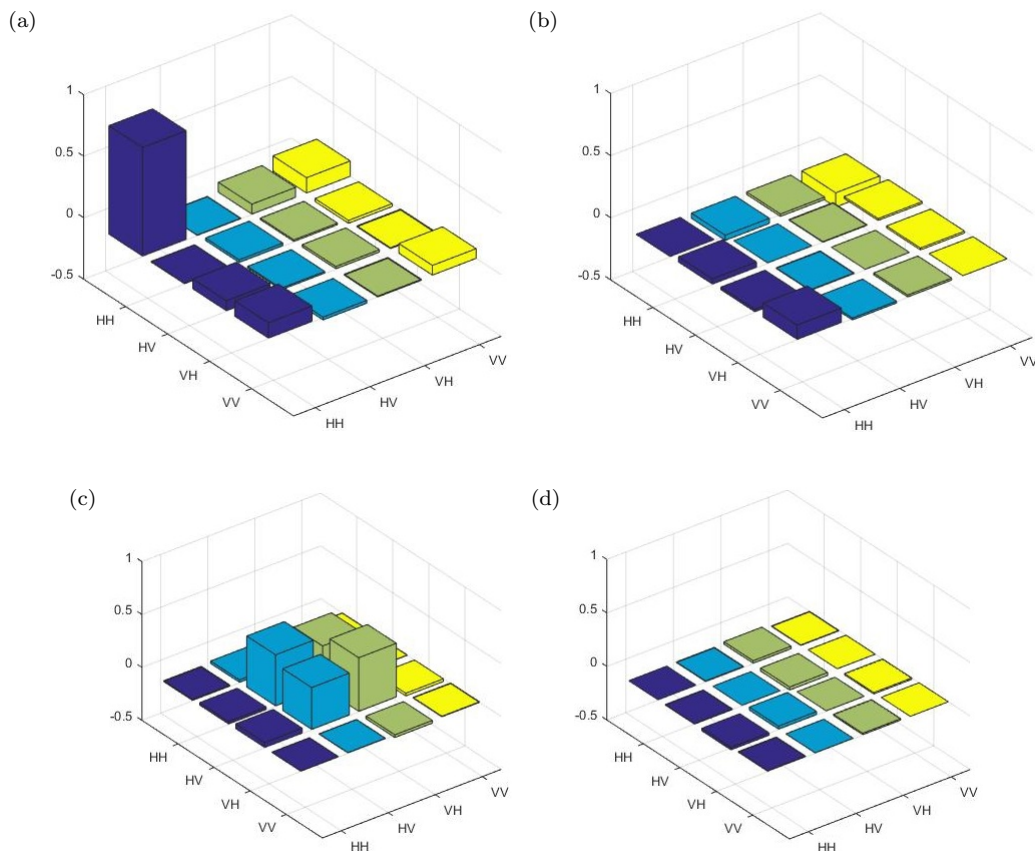


Figure 4.8: **Density matrices for the population difference of 0.7720.** 4.8a and 4.8b are the real and imaginary parts of the polarization tomography, respectively, that is, before any operation is applied. 4.8c and 4.8d are the real and imaginary part of the momentum state, respectively, after the filtering. In this two later cases path information was transformed into polarization information, therefore polarization H means path u and polarization V means path d . The path and polarization matrices present data on different spots because in polarization the correlation is between qubits with the same information on both sides ($|HH\rangle$ or $|VV\rangle$), while in path the correlation is between qubits with different information in each side ($|ud\rangle$ or $|du\rangle$)

In addition to state tomography, the assemblages were also reconstructed and analysed using MatLAB based on codes from Daniel Cavalcanti *et al* [35] using the projective measurements performed on path and polarization. From these measurements we built the assemblages, where the original assemblage was obtained from coincidences in polarization projections, because it represent photons that did not undergo any filtering, and the filtered assemblage was obtained from coincidences in path projections. From the assemblages we obtained the following steering robustnesses

Pop. Difference	Assemblage	SR
0.2156	Original	0.08 ± 0.02
	Filtered	0.10 ± 0.02
0.5079	Original	0.11 ± 0.01
	Filtered	0.12 ± 0.02
0.6042	Original	0.09 ± 0.01
	Filtered	0.14 ± 0.01
0.7720	Original	0.02 ± 0.01
	Filtered	0.11 ± 0.02

Tabela 4.1: Values found for the steering robustness of the original assemblage (path measurements before the local operation) and the filtered assemblage (path measurements after the local operation).

where the uncertainty is obtained via the standard deviation of robustnesses calculated from a poissonian distribution of coincidence counts, generated via Monte Carlo simulation. Using the values for the robustness we can make a comparison between the original assemblage and the filtered one. The expected result is that the original assemblages would be less steerable when compared to those which undergo filtering. Another important analysis is to compare the experimental data obtained and the expected theoretical values (see Figure 4.9). In this analysis, we calculated the SR for the theoretical initial and final state both before and after distillation, respectively. However, to obtain a better comparison with our experimental data, we considered the state with 7.5% dephasing. We chose this value based on the reduction in the coherences observed in the tomography of our states.

Based on Table 4.1 and Figure 4.9, we can clearly observe that every filtered assemblage (blue square points) have a greater SR value than their respective original assemblage (red square points), indicating that the distillation process was successful. One important point to notice in Figure 4.9 is that, in the case of $PD = 0.2156$, the SR for the filtered assemblage was not greater than that for the polarization. This does not discredit the distillation, however, in a practical implementation of this scheme, it would not be efficient to use the path assemblage in place of the polarization.

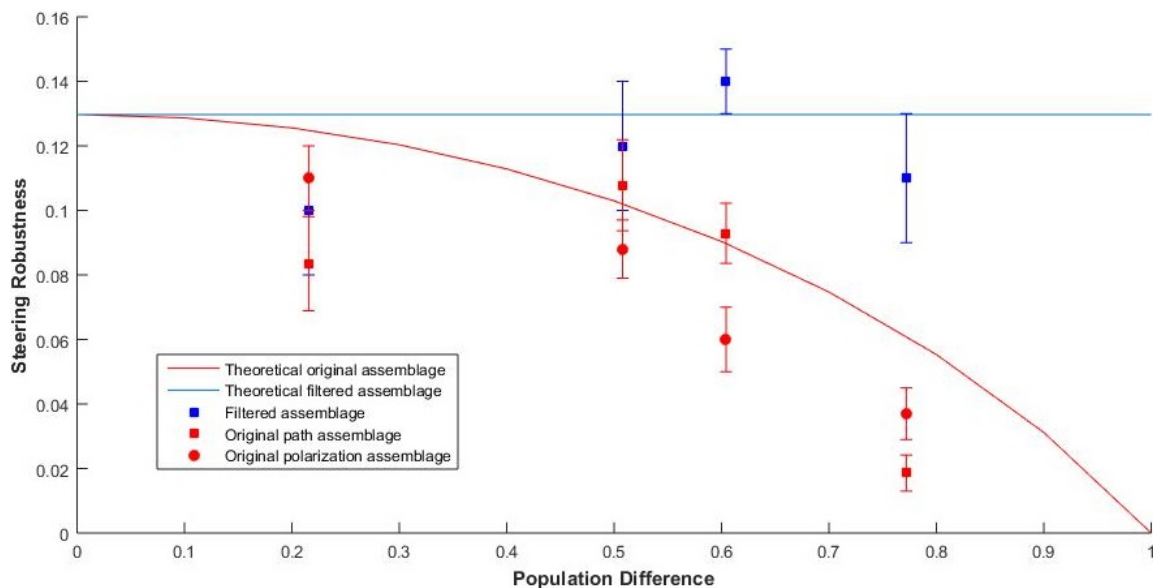


Figure 4.9: **Steering robustness values.** The curves correspond to a theoretical simulation with 7.5% of dephasing from a pure assemblage. The constant curve (blue) is the filtered assemblage, which always has the highest steerability, because it represent a perfectly distilled assemblage. The lower curve (red) is the original assemblage, with no filtering. The points were obtained from the experiment, where the blue square points are from the distilled assemblage, the red square points are from the path measurements before distillation and the red circle points are from the polarization measurements.

As a certification procedure to guarantee the presence of a shared quantum state we calculated the entanglement negativity [40] of the states using the QETLAB Toolbox⁵ (see Figure 4.10). The negativity is an entanglement monotone used as a measure of quantum entanglement and is defined as

$$\mathcal{N}(\rho) \equiv \frac{\text{Tr} |\rho^{\tau A}| - 1}{2} \quad (4.10)$$

where $\rho^{\tau A}$ is the partial transpose of ρ with respect to the system A and $\text{Tr} |\rho^{\tau A}|$ is the trace norm. If the negativity is greater than zero ($\mathcal{N} > 0$), the state is entangled. On the contrary, the state is separable. This serves to confirm that the states are entangled, and even more, shows that for most cases the filtered states contain a higher degree of entanglement than the original ($\mathcal{N}_{\text{Filt.}} > \mathcal{N}_{\text{Original}}$).

⁵The Quantum Entanglement Theory LABoratory toolbox is a MATLAB toolbox containing several operations used in quantum entanglement theory

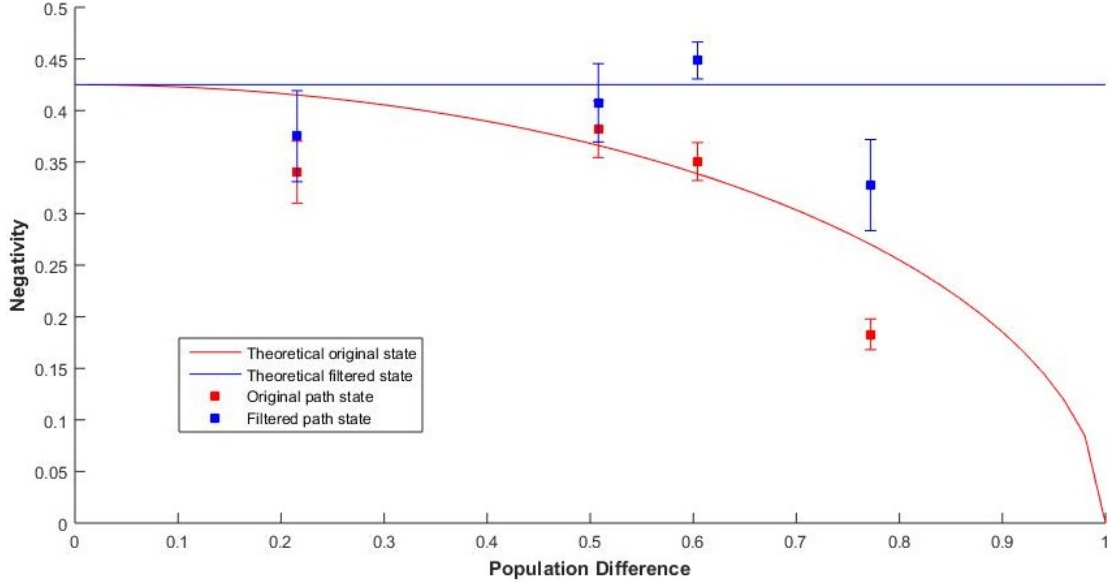


Figure 4.10: **Negativity values for the original and filtered states.** The curve correspond to the theoretical results, while the points are from the experiment. Red circular points are the original state and blue square points are filtered states. A maximally entangled state has a negativity of 0.5, but in our analysis there is a 7.5% dephasing, which lowers the negativity curve.

Figure 4.10 shows that the negativity for the original entangled states (red square points) was increased by the local filtering operation (blue square points). Demonstrating entanglement distillation is an important result because, although it was not our first goal, it is the first time a hyper-entangled state is used to demonstrate distillation in a deterministic way, that is, an entangled state with at least the same amount of entanglement as the original state is produced for all pair of photons.

Our experiment is a proof-of-principle, in the sense that Bob actually does not communicate the result of his measurement (path or polarization) to Alice. Moreover, Bob only learns whether the filtering operation worked or not when he detects his photon. Still, the present scheme (with communication to Alice) could be used for protocols such as quantum key distribution, where only local measurements are performed.

The results presented above correspond to a first set of measurements. Next steps include repeating the experiment for a wider set of original states, and extending our approach to more complex filtering schemes, possibly involving joint measurements on both copies of Bob's qubits.

Chapter 5

Conclusion and remarks on future work

The present experiment had the goal to demonstrate an scheme to distill quantum steering. In the end, we showed that, with two copies, it is possible to achieve steering distillation in a deterministic fashion. For distillation, we use two copies of a bipartite state of qubits encoded into a single pair of photons. These are known as hyper-entangled photon states, representing the fact that simultaneous entanglement in multiple degrees of freedom is present. Our experiment can then perhaps be seen as a distillation of hyper-entanglement to entanglement. The price one pays to do this is that sometimes the momentum degree of freedom is used for the output state, other times the polarization degree of freedom. However, when we use the momentum state, we transform the momentum entanglement to polarization degree of freedom as part of our measurement procedure. Thus, the output state is always in the polarization degree of freedom of the photon pair.

To respect the requirements of the resource theory of steering it was necessary to perform a protocol using only 1W-LOCC operations, where in our case Bob is allowed to perform local measurements on his quantum system and communicate to Alice. In the protocol, Bob performs a local filtering operation on one of his qubits. If successful, the steering of the output state is increased. If not successful, the steering is zero, and the second pair of qubits is then used. On average, steering is increased in this process. A future direction of theoretical and experimental research would be to study steering distillation protocols where Bob performs measurements on both of his qubits.

An extension of the present work for future research would be distillation with a higher number

of copies. However, distillation with two copies is already enough to optimize protocols of quantum communication and cryptography. In the latter, steerable states can be used to generate a secret key for communication, and the number of cryptographic keys successfully established is higher as higher the steerability is. Also, as correlated photons travel through a channel they can suffer decoherence, leading to a loss of efficiency of the communication. Distillation can help this process by increasing the steerability after the photons have exited the channel. These benefits provided by highly steerable states are very important for operations where you trust one system but cannot make any assumption about a second party's system. One example of such systems is a bank communication, where banks can afford a complete trustworthy (= expensive) device, but has to communicate with its clients, who not necessarily can afford a trusted device.

References

- [1] A. Einstein, B. Podolsky, and N. Rosen. Can quantum-mechanical description of physical reality be considered complete? *Physical Review*, 47:777–780, 1935.
- [2] J. S. Bell. On the einstein podolsky rosen paradox. *Physics*, 1(3):15, 1964.
- [3] Reinhard F. Werner. Quantum states with einstein-podolsky-rosen correlations admitting a hidden-variable model. *Physical Review A*, 40(8):4277–4281, 1989.
- [4] V. Vedral and M. B. Plenio. Entanglement measures and purification procedures. *Nature Physics*, 4:873–877, 2008.
- [5] Guifré Vidal and Rolf Tarrach. Robustness of entanglement. *Physical Review Articles*, 59:31, 1999.
- [6] Ryszard Horodecki, Pawel Horodecki, Michal Horodecki, and Karol Horodecki. Quantum entanglement. *Rev. Mod. Phys.*, 81:865–942, 2009.
- [7] E. Schrödinger. Discussion of probability relations between separated systems. *Mathematical Proceedings of the Cambridge Philosophical Society*, 31:555–563, 1935.
- [8] H. M. Wiseman, S. J. Jones, and A. C. Doherty. Steering, entanglement, nonlocality, and the einstein-podolsky-rosen paradox. *Physical Review Letters*, 98:4, 2007.
- [9] Cyril Branciard, Eric G. Cavalcanti, Stephen P. Walborn, Valerio Scarani, and Howard M. Wiseman. One-sided device-independent quantum key distribution: Security, feasibility, and the connection with steering. *Phys. Rev. A*, 85:7, 2012.
- [10] Rodrigo Gallego and Leandro Aolita. The resource theory of steering. *Physical Review X*, 5:19, 2015.
- [11] Paul Skrzypczyk, Miguel Navascués, and Daniel Cavalcanti. Quantifying einstein-podolsky-rosen steering. *Physical Review Letters*, 98:4, 2014.

- [12] Marco Piani and John Watrous. Necessary and sufficient quantum information characterization of einstein-podolsky-rosen steering. *Physical Review Letters*, 114:6, 2015.
- [13] Charles H. Bennett and Stephen J. Wiesner. Communication via one- and two-particle operators on einstein-podolsky-rosen states. *Phys. Rev. Lett.*, 69:2881–2884, 1992.
- [14] Dik Bouwmeester, Jian-Wei Pan, Klaus Mattle, Manfred Eibl, Harald Weinfurter, and Anton Zeilinger. Experimental quantum teleportation. *Nature*, 390:575–579, 1997.
- [15] Charles H. Bennett and Gilles Brassard. Quantum cryptography: Public key distribution and coin tossing. *International conference on computer, systems & signal processing*, 1:173–179, 1984.
- [16] Charles H. Bennett and Gilles Brassard. Quantum cryptography: Public key distribution and coin tossing. *Theoretical computer science*, 560:7–11, 2014.
- [17] Artur K. Ekert. Quantum cryptography based on bell’s theorem. *Phys. Rev. Lett.*, 67:661–663, 1991.
- [18] Richard Cleve and Harry Buhrman. Substituting quantum entanglement for communication. *Phys. Rev. A*, 56:1201–1204, 1997.
- [19] Jonathan Barrett, Lucien Hardy, and Adrian Kent. No signaling and quantum key distribution. *Phys. Rev. Lett.*, 95:4, 2005.
- [20] A. J. Bennet, D. A. Evans, D. J. Saunders, C. Branciard, E. G. Cavalcanti, H. M. Wiseman, and G. J. Pryde. Arbitrarily loss-tolerant einstein-podolsky-rosen steering allowing a demonstration over 1 km of optical fiber with no detection loophole. *Phys. Rev. X*, 2:12, 2012.
- [21] Bernhard Wittmann, Sven Ramelow, Fabian Steinlechner, Nathan K. Langford, Nicolas Brunner, Howard M. Wiseman, Rupert Ursin, and Anton Zeilinger. Loophole-free einstein-podolsky-rosen experiment via quantum steering. *New Journal of Physics*, 14:12, 2012.
- [22] Paul G. Kwiat, Salvador Barraza-Lopez, André Stefanov, and Nicolas Gisin. Experimental entanglement distillation and ‘hidden’ non-locality. *Nature*, 409:1014–1017, 2001.
- [23] Paul G. Kwiat. Hyper-entangled states. *Journal of Modern Optics*, 44(11-12):12, 1997.
- [24] Julio T. Barreiro, Nathan K. Langford, Nicholas A. Peters, and Paul G. Kwiat. Generation of hyperentangled photon pairs. *Physical Review Letters*, 95:4, 1998.

- [25] Richard Jozsa. Fidelity for mixed quantum states. *Journal of modern optics*, 41:2315–2323, 1994.
- [26] Andrew G. White, Daniel F. V. James, Philippe H. Eberhard, and Paul G. Kwiat. Nonmaximally entangled states: Production, characterization, and utilization. *Physical Review Lett.*, 83(16):3103–3107, 1999.
- [27] Robert W. Boyd. *Nonlinear Optics*. Elsevier Inc., 2008.
- [28] Paul G. Kwiat, Edo Waks, Andrew G. White, Ian Appelbaum, and Philippe H. Eberhard. Ultrabright source of polarization-entangled photons. *Physical Review A*, 60(2):773–776, 1999.
- [29] Julio T. Barreiro, Tzu-Chieh Wei, and Paul G. Kwiat. Beating the channel capacity limit for linear photonic superdense coding. *Nat. Phys.*, 4:282–286, 2008.
- [30] Stephen P. Walborn. Breaking the communication barrier. *Nat. Phys.*, 4:268–269, 2008.
- [31] Daniel J. Gauthier, Christoph F. Wildfeuer, Hannah Guilbert, Mario Stipcevic, Bradley G. Christensen, Daniel Kumor, Paul Kwiat, Kevin T. McCusker, Thomas Brougham, and Stephen Barnett. Quantum key distribution using hyperentangled time-bin states. *Conference on Coherence and Quantum Optics*, W2A-2, 2013.
- [32] Berthold-Georg Englert, Christian Kurtsiefer, and Harald Weinfurter. Universal unitary gate for single-photon 2-qubit states. *Phys. Rev. A*, 63:10, 2001.
- [33] Daniel F. V. James, Paul G. Kwiat, William J. Munro, and Andrew G. White. Measurement of qubits. *Physical Review A.*, 64:15, 2001.
- [34] E. Schrödinger. Probability relations between separated systems. *Mathematical Proceedings of the Cambridge Philosophical Society*, 32:446–452, 1936.
- [35] Daniel Cavalcanti and Paul Skrzypczyk. Quantum steering: a review with focus on semidefinite programming. *Rep. Prog. Phys.*, 80:31, 2017.
- [36] Charles H. Bennett, Herbert J. Bernstein, Sandu Popescu, and Benjamin Schumacher. Concentrating partial entanglement by local operations. *Phys. Rev. A*, 53:2046–2052, 1996.
- [37] Charles H. Bennett, Gilles Brassard, Sandu Popescu, Benjamin Schumacher, John A. Smolin, and William K. Wootters. Purification of noisy entanglement and faithful teleportation via noisy channels. *Phys. Rev. Lett.*, 76:722–725, 1996.

- [38] Jian-Wei Pan, Christoph Simon, Caslav Brukner, and Anton Zeilinger. Entanglement purification for quantum communication. *Nature*, 410:1067–1070, 2001.
- [39] Vladimir B. Braginsky, Yuri I. Vorontsov, and Kip S. Thorne. Quantum nondemolition measurements. *Science*, 209:547–557, 1980.
- [40] G. Vidal and R. F. Werner. Computable measure of entanglement. *Phys. Rev. A*, 65:11, 2002.

Appendix A

Measurement outcome

Table containing the measurements outcome for a path tomography. Here $\alpha/\beta = 9$ and the filtering is set to make $\gamma' = \delta'$.

	Coincidence counts		
Alice/Bob Projection	Alice's path/Bob's path side	Alice's path/Bob's polarization side	Total coincidences
VV	2	4	6
HV	201	898	1099
RV	102	458	560
DV	106	385	491
DH	138	433	571
RH	91	459	550
HH	2	878	880
VH	212	12	224
VR	115	15	130
HR	107	887	994
RR	187	476	663
DR	106	417	523
DD	198	428	626
RD	102	494	596
HD	108	894	1002
VD	95	10	105

Appendix B

Equipment

List of all optical equipments used on the experiment.

Optical element	Company	Model	Description
Laser	Kimmon Koha Co., Ltd.	IK	50mW, HeCd laser, $\lambda = 325$ nm
Waveplates	Thorlabs		$\lambda = 325$ nm
	Thorlabs	WPH05M-633	Zero order, HWP, $\lambda = 633$ nm
	Thorlabs	WPQ05M-633	Zero order, QWP, $\lambda = 633$ nm
Mirrors	Thorlabs	BB1-E02	25,4 mm diameter, $\lambda = 400 - 750$ nm
Variable Mirror	Thorlabs	NDL - 25C - 4	25mm x 100mm, ND Filter
Beam displacer	Altechna Co. Ltd.	2-BD-CALC-88-3	Calcite crystal
Polarizing beamsplitter	Thorlabs	PBS202	$\lambda = 620 - 1000$ nm
Coupler	Newport	M 20x	0.4
Optical fibre	Thorlabs	P1-780A-FC-2	Monomode, 2 m length $\lambda = 633 - 680$ nm
Single photon detector	PicoQuant	τ -SPAD	< 350 ps resolution, 70% efficiency
FPGA	National Instruments		